Received: 23 November 2022 | Revised: 24 October 2023 | Accepted: 23 November 2023

DOI: 10.1111/maec.12785

RESEARCH ARTICLE

marine ecology WILEY

Algal cover as a driver of diversity in communities associated with mussel assemblages across eastern Pacific ecoregions

Lynn Wilbur[1] | Frithjof C. Küpper[1,2,3] | Vasilis Louca[1]

[1]School of Biological Sciences, University of Aberdeen, Aberdeen, UK

[2]Marine Biodiscovery Centre, Department of Chemistry, University of Aberdeen, Aberdeen, UK

[3]Department of Chemistry and Biochemistry, San Diego State University, San Diego, California, USA

Correspondence
Vasilis Louca, School of Biological Sciences, University of Aberdeen, Cruickshank Building, St. Machar Drive, Aberdeen AB24 3UU, UK.
Email: v.louca@abdn.ac.uk

Funding information
Marine Alliance for Science and Technology for Scotland, Grant/Award Number: HR09011

Abstract

Research on intertidal mussel assemblages and associated communities has revealed that complexity and structure are influenced by environmental heterogeneity and local-scale factors affecting recruitment. Research in situ in eastern and western Pacific intertidal ecosystems has suggested drivers of species diversity and community structure encompassing large geographic scales, however, there are major gaps in geographic coverage. Our aim is to fill some of these gaps by analyzing macrofaunal functional group diversity and effects of environmental factors on intertidal mussel communities from three distinct marine ecoregions in the southern and northern hemispheres. We identified the effects of algal cover and environmental heterogeneity on species richness and evenness, and we modeled factors effecting mussel layer complexity from assemblages in three marine ecoregions. We analyzed macrofaunal species diversity within one of the austral ecoregions based on the width of the coastal shelf. Species richness was highest in samples from the northern hemisphere while evenness was highest in samples from the southern hemisphere. Similarity in functional group structure for all communities sampled was ≤55% (Bray–Curtis dissimilarity) and ≤35% (Chao–Jaccard dissimilarity). Wave exposure had a significant effect on shell length and complexity of mussel matrices on rocky bench platforms. The presence of algal cover had a strong effect on species richness in mussel matrices regardless of complexity, while algal canopies had no effect on species evenness. Overall, this study provides significant new insight on the community complexity of mussel beds in parts of the world which have been poorly studied in this regard.

KEYWORDS
algal cover, intertidal communities, marine ecoregion, mussel assemblages, mussel matrix, species richness, wave exposure

1 | INTRODUCTION

Mussels have been described as "bioengineer species" with significant linkages to species richness and evenness based on shell size, age-class, stratification of various age-classes of mussels, and the presence of algal epibionts (Alvarado & Castilla, 1996; Firstater et al., 2011; Guiñez & Castilla, 1999; Prado & Castilla, 2006). In dynamic marine ecosystems such as intertidal and shallow subtidal areas,

algal cover functions as macro-scale habitat that defines community structure and provides a buffer from local climate extremes essential for a variety of intertidal species including mussels (Bulleri et al., 2002; Jenkins et al., 1999; Leite et al., 2021; Leonard, 1999; Stachowicz et al., 2008). It is in this extreme environment assemblages of intertidal mussels are exposed to the limits of their temperature thresholds (Helmuth et al., 2006; Szathmary et al., 2009; Williams et al., 2008). For example, during periods of extreme low tides when the intertidal zone is exposed for several hours, algal cover provides protection from desiccation and other effects from environmental extremes to under-story mussel communities (Prado & Castilla, 2006; Stachowicz et al., 2008; Storero et al., 2022; Valdivia, Aguilera, & Broitman, 2021; Valdivia, López, et al., 2021). Furthermore, there is evidence to suggest that the presence of canopy-forming algae influences the rates of recruitment and settlement of other algal species (Benedetti-Cecchi et al., 1996), barnacles (Leonard, 1999), and potentially, marine mussels as well. Bulleri et al. (2002) found that the experimental removal of canopies of *Cystoseira* resulted in an increase in branched algal and coralline species that corresponded with the disappearance of many other species. At the same time, potential interactions between algal cover and mussel species can be two-directional; Benedetti-Cecchi et al. (1996) demonstrated that the removal of mussels resulted in an increase in algal canopy likely due to the inhibitory effect of the mussels on algal recruitment.

The intertidal environment is highly variable in terms of temperature and radiation, and research on the physiological responses of mussels to environmental stress suggests that mussels in any given geographic range have developed adaptations that enable them to survive within certain limits (Helmuth et al., 2006; Szathmary et al., 2009). Due to their suitability as substrate in hard and soft bottom intertidal environments (Prado & Castilla, 2006; Thiel & Ullrich, 2002; Valdivia, Aguilera, & Broitman, 2021), mussel assemblages are ideal for measuring the diversity of macro-scale communities associated with them and thus the importance of addressing factors that mitigate the impacts from environmental stressors cannot be overstated, particularly when assessing mussel community diversity and hierarchical structure (Harley & Helmuth, 2003). The physiological adaptations attributed to various mussel species have explained temperature and desiccation tolerances to some degree, however, the wetting provided by ocean waves plays a significant role in mitigating heat stress when mussels living near their upper-temperature thresholds (Dahlhoff & Menge, 1996; Harley & Helmuth, 2003). For example, the orientation of mussel assemblages along the shore in a temperate region may serve to mitigate upper-temperature extremes brought about by small-scale changes in climate (Dahlhoff & Menge, 1996; Helmuth et al., 2006; Konar et al., 2010). Ocean waves play a role in the availability of nutrients along the shoreline as well as phytoplankton abundance and have been significantly linked to higher primary productivity, higher metabolic activity in mussels (Dahlhoff & Menge, 1996; Menge, Daley, Wheeler, Dahlhoff, et al., 1997; Menge, Daley, Wheeler, & Strub, 1997), and size distributions and recruitment of juvenile mussels (Alvarado & Castilla, 1996). Local-scale high primary productivity following nutrient delivery in shallow coastal areas has the potential to trigger bottom-up trophic cascades, which in turn facilitates the settlement of various planktotrophic macro-invertebrates onto suitable hard substrate in the intertidal zone such as the shells of mussels. Small-scale patterns in community structure may also be attributed to wave exposure while also taking into consideration other variables such as top-down effects (Dahlhoff & Menge, 1996; Menge, 1992; Menge, Daley, Wheeler, Dahlhoff, et al., 1997; Menge, Daley, Wheeler, & Strub, 1997).

Ocean waves also serve as a dispersal mechanism for marine algae and facilitate the transport of algal sporelings throughout their vertical range in the intertidal zone (Harley & Helmuth, 2003). The shells of intertidal mussels provide substrate for the thalli of seaweeds to anchor and where mussels are abundant, algae may form expansive upper-story canopies. Temperature and desiccation are the primary limiting factors for successful algal sporeling recruitment in the high intertidal zone while herbivore abundance and competition for space are primarily the limiting factors in the lower intertidal (Steneck & Dethier, 1994; Underwood & Jernakoff, 1984). Species of canopy-forming seaweeds found higher in the intertidal have been characterized as "drought resistant" as a result of surface to volume ratio of the blades, complex cellular structure, and lipid content; examples include the leathery macrophyte *Fucus* and the corticated macrophyte *Ahnfeltia* spp. (De Vogelaere & Foster, 1994; Schonbeck & Norton, 1979). Prado and Castilla (2006) found that algal canopies played a significant role in species richness in mussel assemblages on the Chilean coast.

Published work on broad-scale marine intertidal diversity has mostly been taken from reviews of the existing literature and mining of historical data from small-scale studies. Only in the past few decades has empirical research been undertaken in an effort to gain a fundamental understanding of species diversity, resilience, and stability in marine intertidal and shallow subtidal meta-communities on local and broad geographic scales (Bryson et al., 2014; Konar et al., 2010; Okuda et al., 2004; Thyrring & Peck, 2021; Valdivia, Aguilera, & Broitman, 2021; Valdivia, López, et al., 2021). Much of the research on mussel-dominated communities in the northern hemisphere has been somewhat limited in scale with a focus on physiological adaptations to heat stress and physical responses to environmental factors (Helmuth, 1998; Menge, Daley, Wheeler, Dahlhoff, et al., 1997), while in the southern hemisphere research has focused on local-scale nutrient uptake and structural complexity of intertidal mussel assemblages (Alvarado & Castilla, 1996; Firstater et al., 2011; Guiñez & Castilla, 1999), with more recent interest in broader-scale surveys (Ibanez-Erquiaga et al., 2018) and evaluation of multi-dimensional stability in intertidal communities associated with mussel assemblages (Valdivia, Aguilera, & Broitman, 2021; Valdivia, López, et al., 2021). Our analysis on the biodiversity of previously unexplored intertidal communities encompassed three distinct marine ecoregions on the Pacific coasts of North and South America and included multiple measures of alpha diversity to account for rare species and relative abundance (Chao et al., 2005; Colwell

et al., 2012; Colwell & Elsensohn, 2014). We tested the effects of environmental variables on the complexity of mussel assemblages, and we tested the hypothesis that there were variations in macrofaunal species richness and evenness in assemblages of *Perumytilus purpuratus* based on environmental and regional factors. Lastly, we examined the degree to which algal cover and wave exposure explained variation in the species composition and diversity of intertidal mussel communities.

2 | MATERIALS AND METHODS

2.1 | The study sites

Marine ecoregions have been described in detail based on homogenous species composition and distinct oceanographic features (Spalding et al., 2007). We selected four sites within the North American Pacific Fjordland (NAPF) ecoregion, two sites within the Guayaquil (GUAY) ecoregion, and eight sites within the Humboldtian ecoregion based on the remoteness of the location, accessibility, relative lack of published research in the proposed field of study, suitable rocky intertidal substrate, and abundance of mussel species endemic to each ecoregion (Figure 1). Various efforts have been undertaken to compare species diversity and evenness in communities associated with mussel assemblages on bio-geographical scales regardless of oceanographic differences and the inter-specific nature of the mussel populations (Buschbaum et al., 2009; Menge et al., 2002). Thiel and Ullrich (2002) found variations in the abundances of specific taxonomic groups in assemblages of *P. purpuratus* at sites separated by 15 degrees of latitude on the Chilean coast, with a directional pattern of abundance in nemertean and polyclad worms. We have divided the Humboldtian ecoregion into two sub-ecoregions (HWS and HNS) based on the relative width of the continental shelf adjacent to the study sites, and similar to Thiel and Ullrich (2002) (see Appendix S1) for non-parametric summaries of mussel matrices in these sub-ecoregions. In order to magnify the spatial resolution of the Humboldtian ecoregion, two divisions are proposed based on the width of the continental margin: the Humboldtian wide-shelf (HWS) ecoregion is approximately 225 km from the edge of the continental shelf to the coastline; and the Humboldtian narrow-shelf (HNS) ecoregion. Three sites were chosen within the HWS sub-ecoregion and five sites were chosen within the HNS sub-ecoregion. Geographic coordinates for the sampling sites and ecoregions can be found in Table 1.

2.2 | Sampling mussel assemblages

We identified mussel species as the target assemblages (Engle, 2008) for each ecoregion. Two species of mussels (family Mytelidae) common to the eastern Pacific of the southern hemisphere are *Perumytilus purpuratus* (Lamarck 1819) and *Semimytilus algosus* (Gould 1850), and both have been studied in regard to species diversity in rocky intertidal communities in Chile (Prado & Castilla, 2006). Dense assemblages of *P. purpuratus* and *S. algosus* are typically found in the high to mid intertidal zone while *S. algosus* and *P. purpuratus* overlap in the mid zone, with *S. algosus* becoming the dominant species in the low zone (Tokeshi & Romero, 2000, L. Wilbur in review). *Brachidontes adamsianus* is the mussel species most commonly encountered in the southern tropical region (A. Pacheco, pers. comm.), and while *P. purpuratus* and *S. algosus* are similar in length at reproductive maturity (Torroglosa & Giménez, 2018), *P. purpuratus* and *B. adamsianus* share similar morphological features (scalloped ridges along the dorsal and ventral valves). *Mytilus trossulus* and *Mytilus californianus* are the two main species of mussels found in the rocky intertidal zone in the eastern Pacific of the northern hemisphere. Evidence of hybridization between the Mediterranean blue mussel *Mytilus galloprovincialis* and *M. trossulus* has been reported for Alaska, however, the distribution of pure stands of *M. trossulus* versus hybridized mussels is not well understood (Burger et al., 2006; McDonald et al., 1991). Another mussel species, *M. californianus*, is typically found in stands of one to a few individuals at or below mean lower low water (MLLW) (Wilbur et al., 2023). Here, we use *Mytilus edulis/trossulus/galloprovincialis* complex (abbr. MytCom) in reference to the mussel species in the NAPF ecoregion (we are following the suggestion of the editors at https://www.centralcoastbiodiversity.org/pacific-blue-mussel-bull-mytilus-trossulus.html).

In the mid to low zone, sessile and motile organisms such as the barnacle *Cthamalus cirrata*, the anemone *Phymactis clematis*, and the chitons *Lucilinia nigropunctata* and *Chiton granosus* recruit on mussel valves of *P. purpuratus* and *S. algosus*, while macro-algae (articulated red algae *Corallina officinalis*, foliose green algae *Ulva rigida*, *Enteromorpha*, and *Colpomenia sinuosa*, and corticated macrophytes belonging to the families Ahnfeltiaceae, Gigartinaceae, and Sarcodiaceae) also recruit as germlings on mussel valves. Sessile and motile invertebrates attach to the valves of these mussel species such as the barnacles *Balanus glandula*, *Semibalanus cariosus*, and the anemone *Metridium senile*, as well as filamentous seaweeds such as *Pterosiphonia bipinnata* and the canopy-forming leathery macrophyte *Fucus gardneri*.

Mussel assemblages were sampled during the austral and boreal summers for each ecoregion: in the NAPF ecoregion between June and July during the years 2017–2018; in the GUAY ecoregion in February 2017; in the HWS ecoregions in February 2017 and in the HNS ecoregion at Reserva Punta San Juan in March (late austral summer) of 2017. Additional mussel assemblage were sampled at Reserva Punta San Juan at N5s and at UOA in March 2018, and at S5 in March 2019. N5n was not sampled in 2018 or 2019 due to extinction of the communities there, and no additional mussel assemblages were sampled in order to avoid bias from re-sampling the same plot, permanent markers were installed as reference points at the highest point in the intertidal zone where biota were first encountered, and all mussels were sampled within the first 10 meters from the highest point in the intertidal zone and to the waterline where the mussels formed an extensive and continuous assemblage. Where mussel assemblages were patchy in distribution

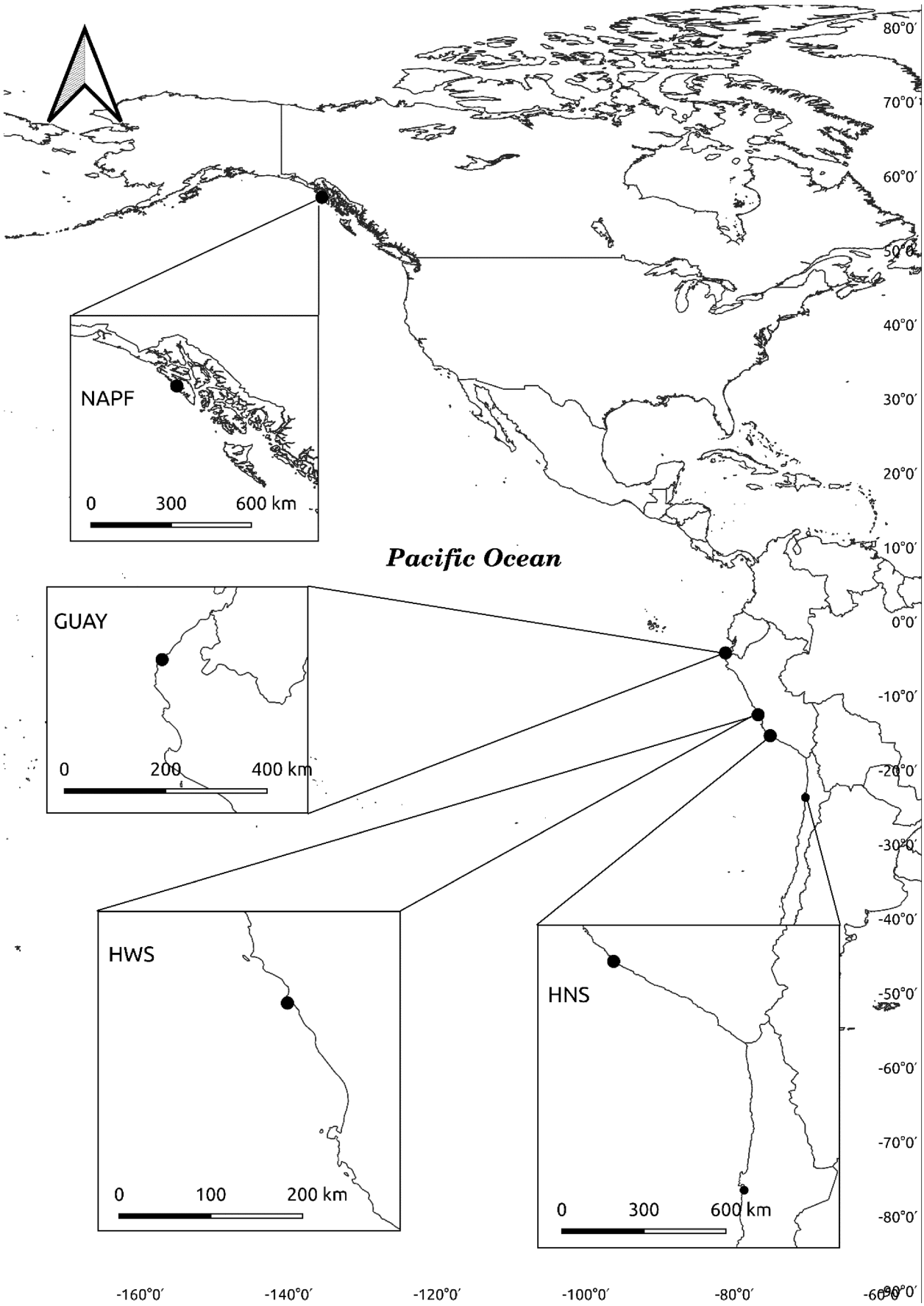

FIGURE 1 Map of the North and South American continents showing the general location of sites selected within each of the marine ecoregions (black dots) with closeups of the shoreline in the area of the study sites indicated in the map insets. Marine ecoregions (from Spalding et al., 2007) are abbreviated as follows: NAPF = North American Pacific Fjordland; GUAY = Guayaquil; HWS = Humboldtian Wide-Shelf; HNS = Humboldtian Narrow-Shelf.

TABLE 1 Geographic coordinates for all ecoregions, sub-ecoregions within ecoregions, and sites within ecoregions and sub-ecoregions where mussel assemblages were sampled for this study.

Ecoregion/site	Latitude	Longitude
Guayaquil (GUAY)	~0° S to 3° S	
Humboldtian	~12° S to 26° S	
Humboltdian Wide-Shelf (HWS)	12°37′ S to 12°58′ S	75°11′ W to 76°40′ W
Playa Ensendada (PEN)	12°38′ S	76°40′ S
Playa Farallones (PFA)	12°44′ S	76°37′51 W
Playa Palmeras (PGA)	12°57′56 S	76°30′ W
Humboldtian Narrow-Shelf (HNS)	15°21′ S to 23′ S	70′ W to 75°11′ W
Reserva Punta San Juan (PSJ)	15°18′ S	75°11′ W
Universidad de Antofagasta (UOA)	23°42′ S	70°25′27
North American Pacific Fjordland (NAPF)	~50° N to 59° N	
Whale Park	57°1′57.72″ N	135°15′1.08″ W
Kayak Island	57°0′30.42″ N	135°21′11.16″ W
Sage Beach	57°3′30.348″ N	135°19′21.36″ W
Pirate's Cove	56°59′13.2″ N	135°22′42.96″ W

(not extensive and continuous), plots were selected where mussel coverage was at least one-third of a quadrat. Compass coordinates and distance from the reference marker to the quadrats were recorded in order to avoid re-sampling. Mussels were sampled by using a stainless-steel spatula to remove a 100 cm^2 area of matrix from the rock within each of the quadrats. The samples were then placed in a shallow pan of seawater for 30 min to allow organisms to emerge from the mussel valves. Organisms ≥1 mm living within and on the mussels were identified and counted using a hand lens and Nikon field 20 × stereoscope (Arakaki et al., 2018, 2019; Dawson et al., 1964; Howe, 1914; Kozloff, 1996; Mendez, 2002; Romero, 2002). Mussel assemblages were sampled at sites within each of the four regions using a 70 cm × 50 cm quadrat strung to provide a grid with 100 intersections (Engle, 2008). Organisms were identified as species or the lowest taxonomic category using reference materials and dichotomous keys. All species were organized into functional groups according to the methods used in Steneck and Watling (1982), that is, invertebrates were categorized by subclass, and algae were categorized by a functional group number according to the level of cellular complexity and physical structure (for definitions of functional groups, see Steneck, 1988; Steneck & Dethier, 1994; Steneck & Watling, 1982).

2.3 | Defining mussel layers

In the intertidal zone where predation and larval recruitment on hard substrates are the limiting factors of space, food web structure, diversity and relative abundance of species associated with these communities have been extensively described (Blanchette et al., 2009; Connell, 1961; Connolly & Roughgarden, 1999; Paine, 1966; Thyrring & Peck, 2021), Mussels in particular have become the focus of research, particularly for their characteristic as a "foundation species," that is, once established, mussels function as biological substrate that increases the area suitable for the recruitment of additional species (Altieri et al., 2007; Alvarado & Castilla, 1996; Wilbur et al., 2023).

Previous studies on mussel shell length, matrix depth, and the area occupied by the matrix have suggested a method using shell length and the area under the matrix to calculate a stratum index for describing mussel matrix complexity, or mussel layering (Guiñez & Castilla, 1999; Hosomi, 1985). Mussel matrix samples were collected independent of the criteria used to define the mussel layers. Shell length and matrix depths were measured within each quadrat, and the appropriate measure of central tendency was calculated based on the distribution of the variables. The total area under the matrix (total occupation area (S)) (Hosomi, 1985) for shell lengths equal to or greater than 10 mm in length was calculated according to the formula

$$S = \left(L^{*}\ 0.1587\right)^{2}$$

and for shell lengths less than 10 mm in length according to the formula

$$S = \left(L^{*}\ 0.555\right)^{1.44}$$

The results from the calculations from each of the raw shell lengths are summed using the formula.

$S = 0.555\ \sum^{n}i = 1\,L^{1.44}\ *\ \text{phi}\ +0.1587\ \sum^{m}i = n+1\,L^{2}\ *\ \text{phi}$ (Hosomi, 1985), where phi is a ratio used to measure body

proportions in plants and animals, and phi = 1.6180339887495. The summed values were used to represent the variable stratum index (SI) for each corresponding plot (Guiñez & Castilla, 1999; Hosomi, 1987). The values for shell length (L), matrix depth (M), and stratum index (SI) for all plots in this study were evaluated for normal distribution of the frequencies with the Anderson-Darling test.

Each plot was categorized as mono-layered or multi-layered based on the median stratum index value calculated for that plot, that is, all plots with a stratum index <2.0 were categorized as mono-layered, and all plots with a stratum index ≧2.0 were categorized as multi-layered. Mono-layered matrices with a stratum index ≤1.00 were categorized as "characteristically mono-layered" according to the mussel assemblage self-thinning theory (Frechette et al., 1992; Guiñez & Castilla, 1999). For comparative analysis, the matrix depths recorded from the macro-faunal and algal sampling were used to define the layers using Prado and Castilla's (2006) classification of mussel matrix layers by measuring the depth of the matrix starting from the topmost mussel to the substrate, with mono-layered matrices defined as ≤2.0 cm in depth and multi-layered matrices defined as >2.0 cm in depth.

2.4 | Scoring algal cover

Treatment designs that include the use of quadrats are particularly effective when used with commonly used measures for describing species diversity across habitat gradients and on multiple scales such as Shannon–Wiener and Simpson's Inverse (Magnussen & Boyle, 1995). Here, we define algal cover according to the methods used in Engle (2008), that is, as a layer of alga covering biota or rock, where rock is the primary substrate for the understory. Biota attached to rock serve as secondary and tertiary substrates for algal canopies, with storied canopies formed by multiple layers of algae. Algal canopies were scored according to Engle (2008) by laying the strung quadrat over the mussel plot and identifying the algae under each of the 100 intersections of the grid on the strung quadrat. Three methods were arbitrarily used to score the plots for cover:

Cover A = a point on the grid where an alga covered primary rock substrate.
Cover B = a point on the grid where an alga covered a secondary invertebrate substrate.
Cover C = a point on the grid where an alga covered a secondary alga substrate.

The scores were then summed and converted to decimal percentages to give the total percent algal cover for each respective plot. When the sums for a mussel plot provided 25% or more coverage, the plot was categorized as "with cover"; plots with less than 25 percent coverage were categorized as "without cover" similar to the definition of cover used in Prado and Castilla (2006).

2.5 | Defining wave exposure and platform angle

Wave exposure was determined qualitatively by assessing the orientation of the mussel plots to open ocean waves and swell similar to the methods used in Dahlhoff and Menge (1996), Menge, Daley, Wheeler, Dahlhoff, et al. (1997), and Menge, Daley, Wheeler, and Strub (1997). Mussel plots that were directly exposed to incoming ocean waves at sites that faced the open ocean were categorized as "wave exposed" and mussel plots that were exposed to waves at an oblique angle, for example on the leeward side of a bay, peninsula, or island, were categorized as "wave sheltered."

The platforms where the mussel plots were sampled were arranged into two categories based on the slope of the substrate; a Häglof EC II D-R clinometer (Häglof Sweden) was used to measure the angle by standing some distance from the platform and sitting at the top of the platform through the clinometer. In general, platforms that were relatively level (the platform could be stood upon) (D'Antonio, 1986) had an angle <45° and were thus categorized as "bench," and platforms that were relatively steep had an angle ≥45° and were thus categorized as "vertical." Where it was difficult to measure the angle of the platform with the clinometer, photographs were used to assess the platform as "horizontal" or "vertical."

2.6 | Diversity analysis

For measuring mean gamma diversity for each ecoregion (for an explanation of mean diversity, please see Colwell et al., 2012, Colwell, 2013), we organized the samples according to species and functional groups and pooled the data by ecoregion. Because of the limited scope of available research on diversity in the mussel communities at the sites, we chose three measures of diversity in order to provide a spectrum of analysis: Shannon–Wiener Index (H) as a standard estimate of species richness and abundance in the samples (Shannon, 1948); Simpson's Inverse Index (1/D) (Simpson, 1949) to evaluate the probability encountering the same species in different samples; and Fisher's alpha (α) because it is sensitive to rare and unique species (Fisher et al., 1943).

One of the difficulties in using the point scoring design for incidence and abundance of species has been accounting for rare and unique species (Chao et al., 2014), thus, we attempted to predict the number of species including those that might be missed during sampling by extrapolating the species richness and then plotting the accumulation curves for each site (Colwell & Coddington, 1994; Peake & Quinn, 1993; Ugland et al., 2003). Two richness methods were used here; species richness (S), or the number of observed species within a given sample and the Chao 1 estimator (S_{Chao1}) for its sensitivity to rare and unique species (Chao, 1984). We used EstimateS software version 9.1 (Colwell, 2013) to graph the accumulation curves from calculated mean richness (S_{sp}) and mean functional group richness (S_{fx}) calculated from each sample using ±95% confidence intervals using randomized re-sampling (bootstrapped to 10^5 samples), with and without replacement (Chao, 1984; Colwell et al., 2012; Colwell

& Elsensohn, 2014). To reduce bias among sample sizes, we rarified the incidence and abundance data for enumerating species richness (Chao, 1987; Colwell et al., 2004).

To compare communities across broad regional scales, we organized the species data into functional groups and evaluated using dissimilarity analyses in the vegan package (Oksanen et al., 2020), RStudio version 1.3.1in the R programming software version 4.0.2 (R Core Team, 2020; RStudio Team, 2020). The Bray–Curtis dissimilarity measure was chosen as a standard that accounts for the most abundant species in a sample (Bray & Curtis, 1957), and the Chao–Jaccard dissimilarity measure was chosen for its sensitivity to rare and unique species (Chao et al., 2005).

2.7 | Statistical analysis

We used multivariate analysis to test the null hypothesis (H_0) that environmental heterogeneity has no effect on the structural complexity of mussel assemblages on the broad geographic scale that we propose. We tested the response variables shell length (L), matrix depth (M), and stratum index (SI) with the pooled explanatory variables, that is, mussel matrices exposed to waves ($n=174$) versus mussel matrices sheltered from waves ($n=104$) and mussel matrices on bench substrate ($n=76$) versus mussel matrices on vertical substrate ($n=202$), and the combined effects of the variables. Exposure and substrate were analyzed as fixed effects. Akaike Information Criterion (AIC) scores were evaluated for models (1) using ecoregion as one random effect, and (2) site and ecoregion as nested random effects. For each respective dependent variable, the model with the lowest AIC score for each random effect or nested random effects was chosen as the best model (Akaike, 1974; Burnham et al., 2011). Ecoregion ($n=4$) and site ($n=14$) were analyzed as nested random effects on the response variables using linear mixed-effects modeling from the lmerTest package (Kuznetsova et al., 2017) in R. The pooled data for each response variable was assessed for normality using the Shapiro–Wilk test. The models with the lowest Akaike Information Criteria scores based on the random effects were chosen. Each linear effects model was then analyzed for significance of variance (Pr (>|f|), $\alpha=.05$) using one-way ANOVA.

The presence of algae and the number of mussel layers as defined by the depth of the matrix has been suggested to play a significant local-scale role in the structure of macrofaunal communities in mussel assemblages (Prado & Castilla, 2006). In order to examine whether diversity could be predicted using the same variables on a broader geographical scale, we parsed the definition of mussel layers based on the method used to define them (stratum index and matrix depth), and we tested the null hypothesis (H_0) that algal cover and mussel layers have no significant effect on species richness and evenness on mussel communities. We organized the mussel layer data into two sets as defined by stratum index or the matrix depth, and we nested the explanatory variables (mono-layered matrices with and without algal cover and multi-layered matrices with and without algal cover). We then pooled the data according to the nested variables, which resulted in non-parametric distributions and unequal populations among pairwise data sets. Methods in non-parametric analysis tend to be lower in power and accuracy for rejecting or accepting the null hypothesis (Siegel, 1957), nevertheless, we used the Wilcoxon rank sum test with 95% confidence intervals (CI) to compare the medians of the sample populations and bootstrapped the confidence intervals to check for variation from the sample CI (Zhou & Dinh, 2005). To reduce bias in species richness introduced by matrices with algal cover, we chose Menhinick's species richness ($I_{Mn}=S/\sqrt{(n)}$) for calculating species richness, where S is the number of species and n is the number of individuals, which effectively provides a standardized index of species richness (Menhinick, 1964). The Pielou's evenness index ($J'=H'/\ln(S)$ where H' is the Shannon Weaver index value and S is the total number of species in the sample) measures equality in the sample population in terms of the number of individuals for each species sampled with the formula. The scale for Pielou's evenness index is from 0 to 1, with numbers closer to 1 indicating higher levels of evenness (Pielou, 1966).

3 | RESULTS

3.1 | Species richness and alpha diversity

A total of 64 species from 12 phyla were sampled from mussel plots in the NAPF ecoregion, with *Fucus gardneri* and *Pterosiphonia bipinnata* the most abundant algal taxa, and members of the genera *Balanus*, *Semibalanus*, *Lottia*, and *Littorina* among the most abundant invertebrate taxa. Thirteen species from six phyla were sampled in mussel plots from the GUAY ecoregion; *Ulva* was the most abundant algal taxon for this ecoregional group. Forty-four species from 11 phyla were sampled from the HWS ecoregion; the green foliose algae *Ulva*, the red crustose algae *Lithothamnion* spp., the polychaete *Perinereis* spp., and the limpet *Scurria* spp. were the most abundant taxa. Finally, 49 species from 11 phyla were sampled from the HNS ecoregion, where *Chondracanthus* spp. was the most abundant algal taxon and *Perinereis* spp., a spionid polychaete (presumed to be *Proboscidia wellingtonensis*), *Echinolittorina* sp., *Scurria* sp., and nemertean worms being the abundant taxa in the mussel communities (Table 2).

Plots of the means for the three measures of diversity computed from randomized resampling of the species and functional group data are shown in Figure 2a–c. Overall, the lowest mean indices were found for the sites sampled within the GUAY ecoregion. When diversity was measured by the proportion of species and functional groups (the Shannon–Wiener Index), the computed indices for communities sampled from the NAPF, HWS, and HNS ecoregions were all within one unit of index, with the highest Shannon–Wiener diversity found for sites within the HWS ecoregion. The probability of encountering similar species and functional groups across samples (the Simpson's Inverse Index) was approximately 1 ½ to 3 times higher in the HWS ecoregion, indicating that species richness and evenness are characteristic of

TABLE 2 Table of species along with raw counts surveyed by sites within ecoregions during the surveys at sites within the NPAF, GUAY, HWS, and HNS ecoregions. Functional algal and taxonomic groups (typically subclass) for each species encountered are listed in the second column of the table.

	North American Pacific Fjordland					
	Algal fx group # or taxonomic group		Kayak Island (KIS)	Sage Beach (SBE)	Pirate's cove (PCO)	Whale Park (WPA)
Chlorophyta						
Chaetomorpha cartilaginea	2	M. Howe, 1914				5
Chaetomorpha sp.	2	Kützing 1845	7	12	1	
Cladophora sp.	2	Kützing 1843		5	3	38
Ulva intestinalis	3	Linnaeus 1753		2		
Ulvaria	3	Ruprecht 1850	9		5	18
Ulva lactuca	3	Linnaeus 1753	2	42		40
Ochrophyta						
Alaria nana	5	H.F. Schrader 1903	2		10	1
Colpomenia peregrina	3.5	Savageau 1927		7		
Ectocarpus sp.	2	Lyngbye 1819	1	10		
Fucus gardneri	5	P.C. Silva 1953	34	134	13	103
Ralfsia sp.	7	Berkeley 1843				3
Scytosiphon lomentaria	3.5	(Lynbye) Link 1833			1	2
Rhodophyta						
Calliarthron tuberculosum	2.5	(Postels & Ruprecth) E.Y. Dawson 1964			4	
Ceramium sp.	2.5	Roth 1797	3			1
Corallina frondescens	6	Postels and Ruprecth 1840			2	
Endocladia muricata	4	(Endlicher) J. Agardh 1847	13	16		2
Hildenbrandia sp.	7	Nardo 1834		1		
Mastocarpus sp.	5	Kützing 1843		1		
Mazzaella sp.	5	G. DeToni 1936		3		
Microcladia borealis	2.5	Ruprecht 1850			1	
Odonthalia floccosa	2.5	(Esper) Falkenberg 1901	14		5	
Pterosiphonia bipinnata	2.5	(Postels & Ruprecht) Falkenberg	42	89	27	13
Plocamium violacea	2.5	Farlow 1877			1	
Polysiphonia hendryi	2.5	N.L. Gardner 1927		7	1	
Polysiphonia hendryi var. compacta	2.5	Hollenberg (Hollenberg) 1961	6	1		2
Halosaccion glanduliforme	3.5	Kützing 1843		12	5	
Nemalion helminthoides	3.5	(Velley) Batters 1902				3
Cnidaria						
Anthopleura xanthogrammica	Hexacoralia	Brandt 1835			2	
Metridium senile	Hexacoralia	Linnaeus 1761	2			
Nematoda						
Nematode sp. not det.	Nematoda			9		4
Platyhelminthes						
Polyclad sp. not. det.	Polycladida		3			1
Nemertea						
Emplectonema gracile	Nemertea	Johnston 1837	1	1	9	1
Nemertea sp. not det.	Nemertea		2			1
Annelida						
Glycera sp.	Errantia	Lamarck 1818	1			

TABLE 2 (Continued)

	North American Pacific Fjordland					
	Algal fx group # or taxonomic group		Kayak Island (KIS)	Sage Beach (SBE)	Pirate's cove (PCO)	Whale Park (WPA)
Nereis sp.	Errantia	Linnaeus 1758	10	2	1	10
Cirratulid sp. not det.	Errantia					1
Mollusca						
Hiatella arctica	Autobranchia	Linnaeus 1767	1			
Littorina scutulata	Caenogastropoda	Gould 1849	4	9	3	39
Littorina sitkana	Caenogastropoda	Phillippi 1846		3	2	2
Lottia asmi	Patellogastrpoda	Middendorff 1848		2	6	2
Lottia digitalis	Patellogastrpoda	Rathke 1833	3	1	5	
Lottia ochracea	Patellogastrpoda	Gould 1846	36	25		11
Lottia paradigitalis	Patellogastrpoda	Fritchman 1960	1	11	3	1
Lottia pelta	Patellogastrpoda	Rathke 1833		2		
Lottia scutum	Patellogastrpoda	Rathke 1833	1			
Lottia sp.	Patellogastrpoda			2		
Nucella ostrina	Caenogastropoda	Gould 1852		2		
Mytilus species complex (MYTCOM)	Autobranchia		x	x	x	x
Arthropoda						
Balanus glandula	Cirripedia	Darwin 1854	10	66	19	94
Amphibalanus sp.	Cirripedia	Darwin 1854	10	13	27	18
Semibalanus cariosus	Cirripedia	Pallus 1788	7	108	26	65
Chthamalus dalli	Cirripedia	Pilsbry 1916		10		
Balanus crenatus	Cirripedia	Bruguière 1789		2		2
Chromopleustes oculatus	Eumalocostraca	Bousfield and Hendrycks 1995	1			
Amphipod sp. *not det.*	Eumalocostraca			7		
Idotea wosnesenskii	Eumalocostraca	Brandt 1851				2
Isopod not. det.	Eumalocostraca		2	1		
Crab, megalops phase			1	1		
Cirolana harfordi	Eumalocostraca	Lockinton 1877	1	9		1
Pagurus hirsutiusculus	Eumalocostraca	Dana 1851		1		
Neomolgus littoralis	Acari	Linnaeus 1758		1		1
Mite sp. not det.	Acari			2		1
Echinodermata						
Cucumaria sp.	Actinopoda	de Blainville 1830			10	
Chordata						
Colonial tunicate sp. *not det.*	Urochordata					1

			Guayaquil		Humboldtian wide-shelf			Humboldtian narrow-shelf				
	Fx #/taxonomic grp.		Playa Acapulco (ACA)	El Nuro (ENU)	Playa Ensenada (PEN)	Playa Farallones (PFA)	Playa Palmeras (PGA)	PSJ N5n	PSJ N5s	PSJ S4	PSJ S5	Univ. Antofagasta (UOA)
Chlorophyta												
Chaetomorpha firma	2	Levring 1941		10								
Ulva rigida	3	C. Agardh 1823		18		1	15	58	28	3	7	7
Ulva lactuca	3	Linnaeus 1753			51							
Cladophora coelothrix	2	Kützing 1843				1	5					
Blue-green algae	1							1	15			
Other green algae undet. sp.								5				

(Continues)

TABLE 2 (Continued)

	Fx #/taxonomic grp.		Guayaquil		Humboldtian wide-shelf			Humboldtian narrow-shelf				
			Playa Acapulco (ACA)	El Nuro (ENU)	Playa Ensenada (PEN)	Playa Farallones (PFA)	Playa Palmeras (PGA)	PSJ N5n	PSJ N5s	PSJ S4	PSJ S5	Univ. Antofagasta (UOA)
Filamentous algae undet. sp.	2									1		
Ochrophyta												
Petalonia fascia	5	(O.F. Müller) Kuntze 1898			8	1				4		
Brown micro-algae	1							4	7			
Rhodophyta												
Hildenbrandia sp.	7	Nardo 1834		5		5						
Ahnfeltia duvillei var. implicata	4	(Kützing) M. Howe, 1914				9	19				1	
Ceramium rubrum	2.5	C. Agardh 1811			1							
Chondracanthus glomeratus	3.5	(Howe) Guiry 1993			17					20	46	
Filamentous red algae undet. sp.	2.5				9		3					
Gigartina sp.	4	Stackhouse 1809			3							
Lithothamnion sp.	7	Heydrich 1897				34	20	2				
Corticated red algae undet. sp.	3.5					1						
Corallina officinalis	6	Linnaeus 1758								5		
Iridaea tuberculosa	4	(J.D. Hooker & Harvey) Grunow 1886								16		
Chondracanthus chammissoi	3.5	(C. Agardh) Kützing 1843									2	
Red algae undet. sp.											14	
Nitophyllum sp.	3.5	Greville 1830										1
Cnidaria												
Phymactis clematis	Hexacoralia	(Drayton in Dana 1846)				87	70					
Anemone undet. sp.	Hexacoralia									13	2	
Nematoda												
Nematode undet. sp.	Nematoda				3	4	3	1		3		
Platyhelminthes												
Polyclad undet. sp.	Polycladia			11	10	2	2			2	5	
Nemertea												
Nemertean undet. sp.	Nemertea					1	3		1		24	27
Annelida												
Phyllodocidae	Errantia	Örsted 1843		2	8							
Glycera sp.	Errantia	Haswell 1879			6	1	3			2	4	1
Nereis sp.	Errantia	Linnaeus 1758			4	3					1	
Perinereis sp.	Errantia	Kinberg 1865			15	8	17			50	4	7
Polynoidae	Errantia	Kinberg 1856			1	3	2					
Serpulidae	Sedentaria	Rafinesque 1815				1						
Syllidae	Errantia	Grube 1850								3	21	1
Oweniidae	Polychaeta							2			1	
Spionidae	Sedentaria	Grube 1850						9	6	15	29	

TABLE 2 (Continued)

			Guayaquil		Humboldtian wide-shelf			Humboldtian narrow-shelf				
	Fx #/taxonomic grp.		Playa Acapulco (ACA)	El Nuro (ENU)	Playa Ensenada (PEN)	Playa Farallones (PFA)	Playa Palmeras (PGA)	PSJ N5n	PSJ N5s	PSJ S4	PSJ S5	Univ. Antofagasta (UOA)
Hesionidae	Errantia	Grube 1850							1			
Mollusca												
Argopecten sp.	Autobranchia	Monterosato 1889				1						
Brachidontes sp.autobranchia	Autobranchia	Swainson 1840	x	x								
Echinolittorina paytensis	Caenogastropoda	Phillipi 1847	6	4					11		16	2
Siphonaria lessoni	Heterobranchia	Blainville 1827		1		3	1				2	
Lottia orbignyi	Patellogastropoda	Dall 1909		4		34	18				6	
Echinolittorina peruviana	Caenogastropoda	Lamarck 1822			1	4	13	23	29	1	57	45
Perumytilus purpuratus	Autobranchia	Lamarck 1819			x	x	x	x	x	x	x	x
Scurria viridula	Patellogastropoda	Lamarck 1819			7	62	20	5	4	56	114	4
Semimytilus algosus	Autobranchia	Gould 1850			20	13	20	1	2			
Stramonita haemostoma	Caenogastropoda	Linnaeus 1767			15		3					
Gastropod undet. sp.					1	2						
Chiton granosus	Neoloricata	Frembly 1827				14	4			9	2	2
Fissurella sp.	Vetigastropoda	Brugiére 1789					2					
Tegula atra	Vetigastropoda	Lesson 1830						1	2	2		
Prisogaster niger	Vetigastropoda									1	1	5
Mussel undet. sp.	Autobranchia									3	25	
Chiton undet. sp.	Neoloricata											1
Incatella cingulata	Caenotgastropoda	G.B. Sowerby I 1825										2
Scurria ceciliana	Patellogastropoda	c'Orbigny 1841										3
Scurria parasitica	Patellogastropoda	c'Orbigny 1841										4
Arthropoda												
Grapsidae	Eumalocostraca									1		6
Cancridae	Eumalocostraca	Latreille 1802			1		1			1		
Isopod	Eumalocostraca	Latreille 1817			1	2	8			6	1	
Decapod undet. sp.							1					
Decapod (megalops phase)					1							
Amphipod							3				1	
Balanus trigonus	Cirripedia	Darwin 1854				1	7					
Chthamalus cirratus	Cirripedia	Darwin 1854				90	x	24	24	19	20	24
Barnacle undet. sp.	Cirripedia						7					11
Ostracod	Ostracoda	Latreille 1802									1	
Porcellanidae	Eumalocostraca	Haworth 1825									4	
Notochthamalus scabrosus	Cirripedia	Darwin 1854	1	18		47		1				1
Bryozoa												
Orange bryozoan undet. sp.						1						
Porifera												
Encrusting sponge undet. sp.						3					1	

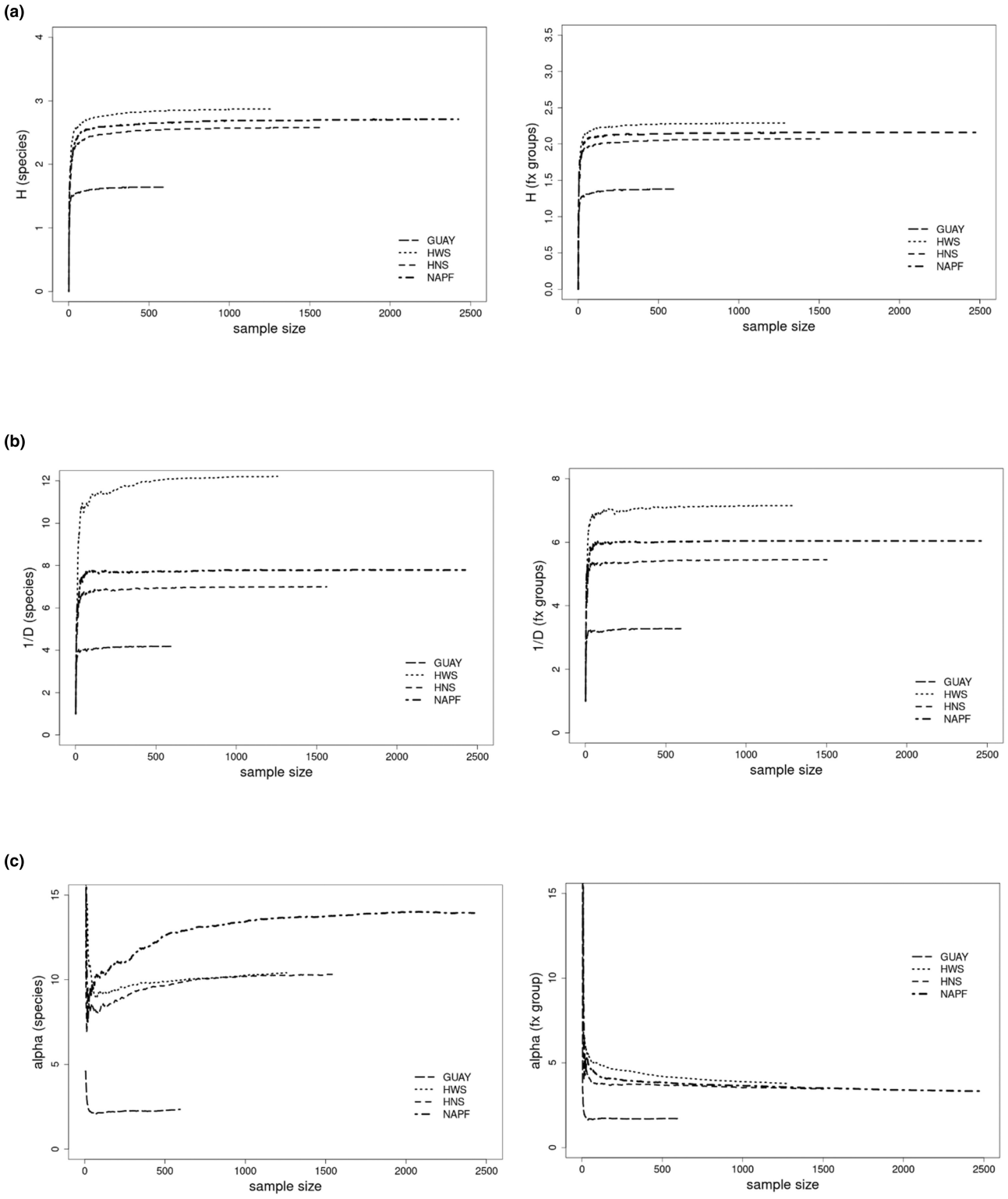

FIGURE 2 (a–c) Sample-size curves of the rarified abundance-based diversity indices from randomized re-sampling of mussel community data from each ecoregion for each of the calculated diversity measures (a) Shannon–Wiener, (b) Simpson's Inverse, (c) Fisher's alpha. Sample data from all ecoregions reached asymptotic richness indices after rarefaction at the minimum sample size of $n = 500$. Total area sampled and number of individuals n are as follows: GUAY: atotal $= 3.85 \times 10^3\,cm^2$ $n = 597$; HNS: atotal $= 1.08 \times 10^6\,cm^2$ $n = 1502$; HWS: atotal $= 5.78 \times 10^5\,cm^2$ $n = 1289$; and NAPF: atotal $= 1.35 \times 10^6\,cm^2$ $n = 2473$. Results for species level analysis are shown in the left column and results for functional group analysis are shown in the right column.

the mussel communities sampled there (Table 3). Mean functional group diversity indices across all measures tended to be lower overall compared to mean species diversity indices, however, the order of ecoregional diversity from lowest to highest remained the same between the two groups. Mean Fisher's alpha diversity, which is sensitive to rare species, was highest for the pooled NAPF sites while Shannon–Wiener and Simpson's inverse was highest for the pooled HWS sites; these rankings may indicate that rare or unique functional groups are an underlying feature of mussel communities at the NAPF sites (Hubbell, 2015), while the higher Shannon–Wiener value for the HWS sites may suggest that functional group richness and evenness is higher in mussel communities there (Strong, 2016). Here, we consider Fisher's α to be useful in this study for approximating diversity at sites that may not have been sampled to completeness given the finite boundaries of the sampling design.

Species accumulation curves for richness S_{Sp}, S_{Fx}, $S_{SpChao1}$, and $S_{FxChao1}$ estimators are shown in Figure 3a–d. Rarefaction

TABLE 3 Mean index values with standard deviations for the three species diversity measures (Shannon–Wiener Index, Simpson's Inverse Diversity Index, and Fisher's alpha diversity index) for mussel assemblage communities sampled at sites within the HWS and HNS sub-ecoregions.

	Species				Functional groups			
Method	Mean	Bootstrapped SD	Lower 95% CI	Upper 95% CI	Mean	Bootstrapped SD	Lower 95% CI	Upper 95% CI
GUAY								
Shannon–Wiener	1.64	0.01			1.38	0.01		
Simpsons Inverse	4.18	0.01			3.28	0.01		
Fishers' alpha	2.35	0.28			1.71	0.22		
S	13.00	2.02	9.03	16.97	10	1.29	7.47	12.53
SChao1	18.99	7.17	13.94	51.05	10.5	1.3	10.03	18.25
Singletons	3.98	0.14			1.99	0.1		
Doubletons	0.01	0.10			0.99	0.1		
HWS								
Shannon–Wiener	2.87	0.01			2.29	0.01		
Simpsons Inverse	12.21	0.01			7.15	0.01		
Fishers' alpha	10.41	0.70			3.77	0.33		
S	50.00	3.31	43.50	56.50	22	0.5	21.03	22.97
SChao1	61.13	8.23	53.05	90.60	22	0.17	22.43	23.1
Singletons	13.02	0.14			1.02	0.14		
Doubletons	5.98	0.14			2	0.1		
HNS								
Shannon–Wiener	2.58	0.01			2.07	0.01		
Simpsons Inverse	7.00	0.01			5.45	0.01		
Fishers' alpha	10.35	0.66			3.46	0.5		
S	52.00	3.36	45.42	58.58	21	0.98	19.09	22.91
SChao1	62.99	8.47	54.88	93.92	21.33	0.93	21.02	26.96
Singletons	12.00	0.14			2	0.14		
Doubletons	5.00	0.14			1.99	0.1		
NAPF								
Shannon–Wiener	2.71	0.01			2.16	0.01		
Simpsons Inverse	7.79	0.01			6.04	0.01		
Fishers' alpha	13.94	0.74			3.33	0.27		
S	72.00	2.82	66.48	77.52	22	0.98	20.08	23.92
SChao1	79.58	5.45	74.14	98.85	23	2.31	22.07	36.32
Singletons	14.02	0.14			1.99	0.1		
Doubletons	10.99	0.17			0.01	0.1		

Note: Mean index values with ±95% confidence intervals for the two species richness measures (Sest and Schao1) along with mean values for singletons and doubletons were calculated using randomized re-sampling with rarefaction in EstimateS v. 9.1 software.

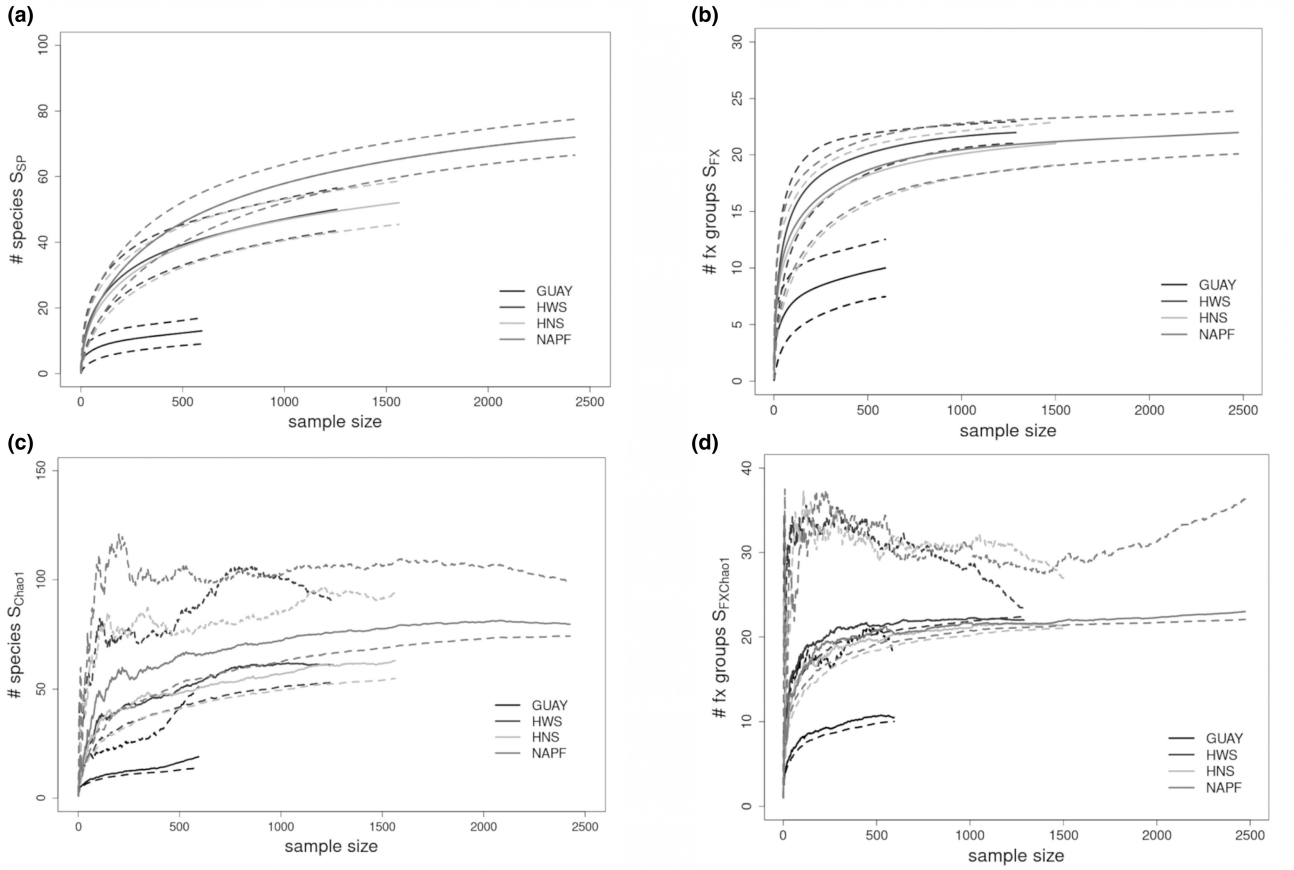

FIGURE 3 (a–d) Rarefaction from randomized re-sampling of the mussel community data at the species-scale (left column) and functional group-scale (right column). Species accumulation curves (solid lines) with 95% confidence intervals (dashed lines) for (a) species-scale richness (SSP), (b) functional group-scale richness (SFX), (c) species-level Chao1 richness (SChao1), and (d) functional-level Chao1 richness (SFXChao1) from mussel community data from each of the ecoregions under study. EstimateS software uses randomized resampling without replacement to calculate S values, while randomized resampling with replacement is used to calculate the SChao1 estimator.

compensates for varying levels of sampling frequency and was employed for both of the species richness estimators used in this study. The re-sampling with replacement design of the S_{Chao1} estimator resulted in higher mean species richness across all ecoregions compared to mean species richness (S), although the S_{Chao1} curve demonstrated a tendency for overestimation of the upper confidence intervals (Chao, 1984). The higher S_{Chao1} values suggested that to a varying degree, rare and unique species were a characteristic among all ecoregions. The S_{SP} and S_{FX} accumulation curves were similar, respectively, in terms of highest to lowest mean values among the ecoregions, with the S_{SP} accumulation curve for GUAY nearing an asymptote at $n = 500$ and the S_{Fx} increasing past $n = 500$. The species richness (S_{Sp}) and functional richness (S_{FX}) curves for the HWS and HNS ecoregions were similar in terms of the richness values and curvilinear feature; S_{sp} continued to increase past $n = 1000$ while the curves representative of the HWS, HNS, and NAPF ecoregions for S_{FX} reached asymptote ~$n = 1000$.

The highest mean values for singletons (species with only one individual in the sample) and doubletons (species with only two individuals in the sample) were calculated for mussel communities sampled at sites within the NAPF ecoregion, while the mussel communities sampled at sites within the HWS ecoregion had the second highest mean singletons (Table 2). Unique and rarely encountered species and functional group taxa at sites sampled in the NAPF ecoregion included the plate limpet *Lottia scutum*, the black and white amphipod *Chromopleustes oculatus*, the polychaete bloodworm *Glyera* spp., the plumose anemone *Metridium senile*, arachnids, corticated macrophytes (fx grp. 5), nemerteans, flatworms, and pyurids; in the HWS ecoregion, the red algae *Ceramium rubrum* and *Gelidium crispum* were rare and unique. In the GUAY ecoregion, rare species and fx group taxa included *Siphonaria* sp. (Dayrat et al., 2014; Güller et al., 2016), two Phyllodocid polychaetes color morphs, red filamentous algae (fx grp. 2.5), heterobranchs, and polychaetes; in the HNS ecoregion, the red alga *Chondracanthus chammissoi*, an Owenid polychaete, an encrusting sponge, green filamentous algae (fx grp. 2), crustose algae (fx group 7), nematodes, nemerteans, and vetigastropods were rarely encountered; and in the HWS ecoregion, the red algae *Ceramium rubrum* and *Gelidium crispum* were rare. In terms of the abundance of herbivorous functional groups in the mussel assemblages, Caenogastropods were abundant in the GUAY ecoregional sites, while caenogastropods, and patellogastropods were equally

abundant in the HNS ecoregional sites. Patellogastropods were the most abundant grazers at sites in the HWS ecoregion, while grazers were relatively less abundant at the sites in the NAPF ecoregion (Figure 4).

3.2 | Multivariate analysis of beta diversity

The mussel *Brachidontes* sp. and the periwinkle *Echinolittorina paytensis* were unique to the GUAY ecoregion, explaining the main dissimilarity among the two sites sampled within that ecoregion and sites within the HWS and HNS ecoregions. Red algae, amphipods, and the limpet Scurria were the species that distinguished the sites within the HWS ecoregion, and the spionid worm (proposed *Proboscidia wellingtonensis*) was a species characteristic of the sites only within the HNS ecoregion. Members of the vetigastropods (turban snails), neoloricata (chitons), and patellogastropoda (limpets), as well as polychaetes were significant functional taxa that differentiated the mussel assemblages within the HNS ecoregion, while functional algal groups 5 (leathery macrophytes) and 2.5 (filamentous red algae) were significant functional taxa that differentiated the mussel assemblages within the NAPF ecoregion. The raw data from all mussel plots were scaled for one nMDS ordination at the functional group level (Figure 5). The general rule for goodness-of-fit between observed and fitted distances and interpreting similarities among communities in an nMDS ordination is to achieve a stress value <0.20 (Rabinowitz, 1975), and in this case, we are confident that the ordination was a fair representation of similarity among sites (stress = 0.13, $k = 2$, p-ANOVA = 0.63). Although there was no overlap among the HNS, HWS, and NAPF clusters, the closeness of the ovoids drawn by the ordination suggests that although the ecoregions are distinct, functional group similarity exists between the HWS and HNS, and to a lesser extent the NAPF ecoregion. Interestingly, site S4 at PSJ shared more similarity with site PFA within the HWS ecoregion than it did within its own HNS cohort. The number of sites sampled within the GUAY ecoregion was insufficient to form a cluster but were included (demonstrated by a one-dimensional line in Figure 5); ACA and ENU were the least similar of all sites within an ecoregional cohort.

Functional algal groups have been ranked in terms of "grazing resistance," with the presence of "structurally tougher" groups linked to increased functional group complexity (Steneck & Watling, 1982). Of the invertebrate functional groups sampled in this study, the caenogastropods (which includes littorinids and dovesnails) were the smallest of the herbivorous grazers in terms of general body size, followed by the patellogastropods (limpets), vetigastropods, (keyhole limpets and turban snails), and neoloricata (chitons). Errant polychaetes, patellogastropods (*Scurria* spp.), vetigastropods (*Fissurella* spp., *Tegula atra*, and *Prisogaster niger*),

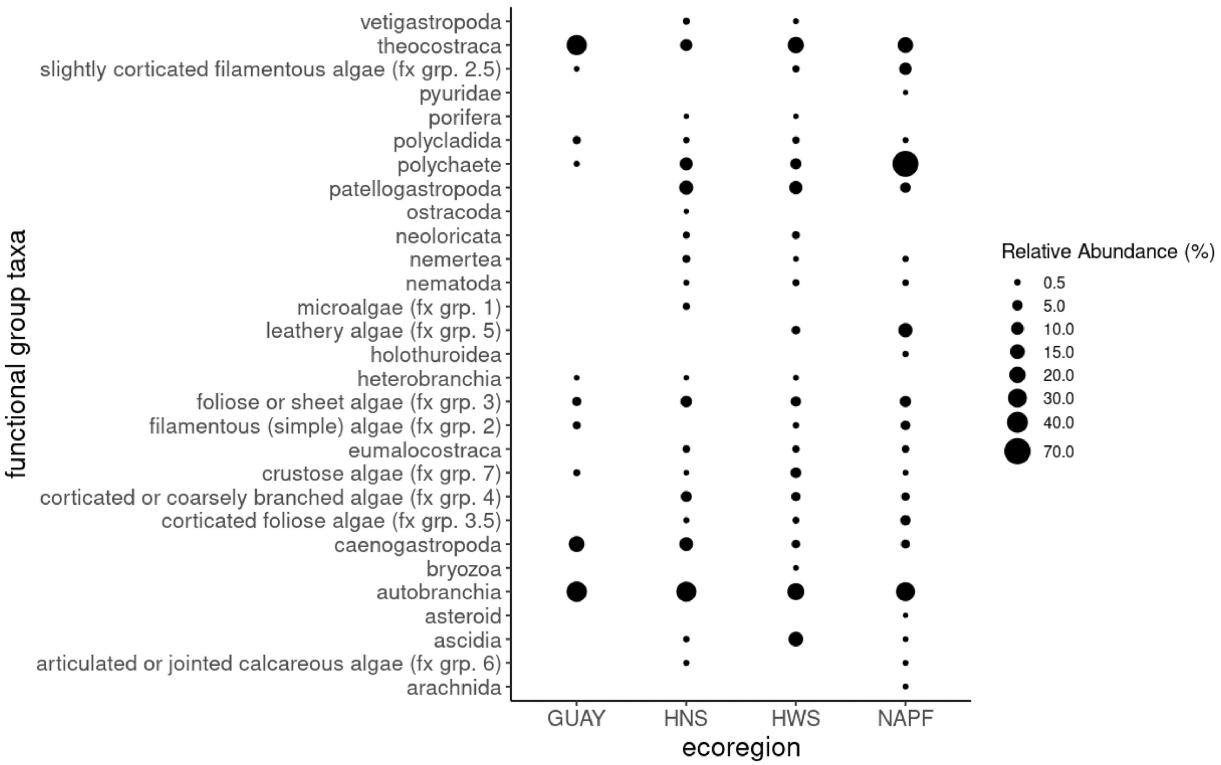

FIGURE 4 Relative abundances of functional group taxa as well as two taxonomic groups (Porifera, Polychaete) associated with mussel assemblages sampled from each of the ecoregions under study. Total area sampled, and no. of individuals calculated for the relative abundances are as follows: GUAY: atotal = 3.85×10^3 cm^2 $n = 597$; HNS: atotal = 1.08×10^6 cm^2 $n = 1502$; HWS: atotal = 5.78×10^5 cm^2 $n = 1289$; and NAPF: atotal = 1.35×10^6 cm^2 $n = 2473$. Functional taxonomic groups are listed according to Steneck (1988).

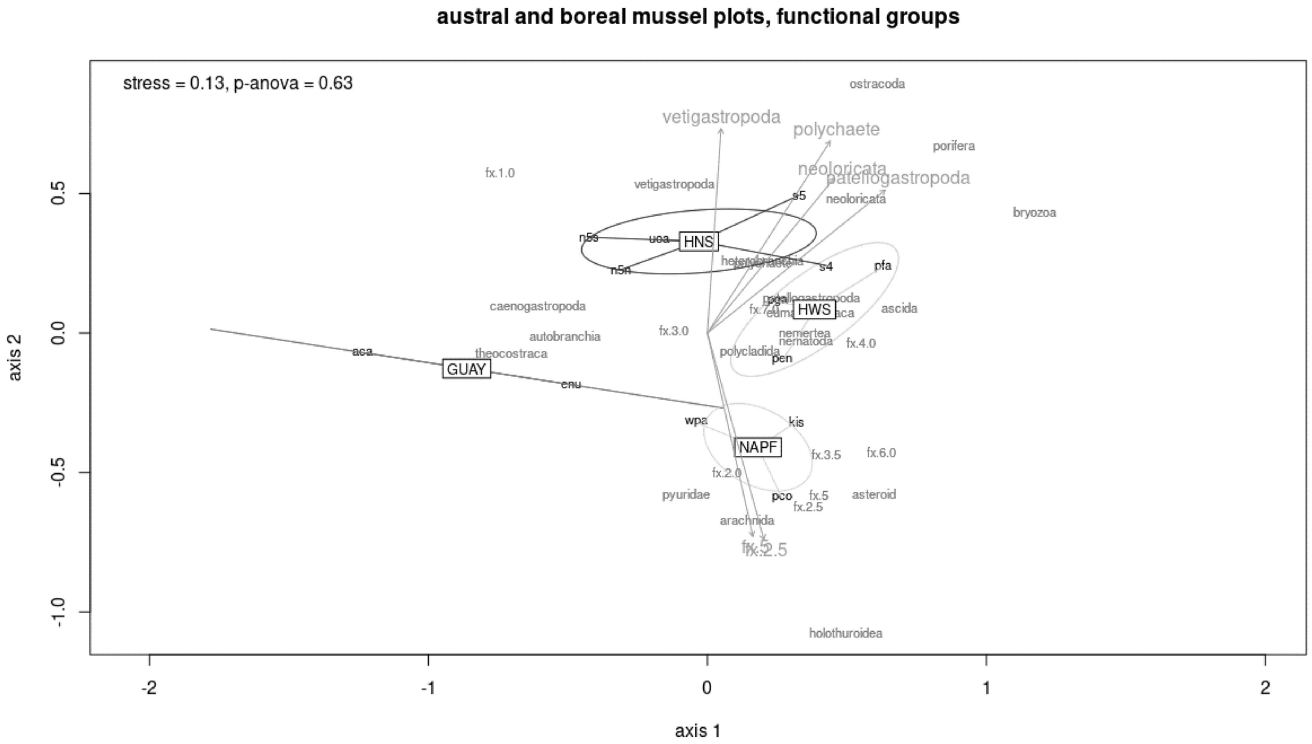

FIGURE 5 nMDS ordinations using Bray–Curtis distance of the functional groups for all mussel plots sampled from all ecoregions (circles) and sites (lines) with stress level and *p*-values from the ANOVA test of the distribution of the data shown in the upper left corner of the graph. Sites are given by abbreviation, refer to Table 1. Light gray arrows point to functional groups with significant fit to the ordination ($p < .05$). Stress values and *p*-values from the ANOVA for dispersal of data shown in the upper left corner of the graph.

and the neoloricata (chitons) were functional groups that were well represented in the mussel communities in the HNS, although errant polychaetes and patellogastropods were also represented to a lesser degree in the HWS. Foliose, crustose, and corticated macrophytes were all well represented in mussel communities within the HWS ecoregion compared to communities within the HNS ecoregion, and in general, mature sporophytes were a common feature in mussel communities within the HWS ecoregion while algal sporelings or small filamentous structures were typical within the HNS ecoregion.

The cluster groups in the dendrograms were similar among all sites from all ecoregions at the functional group level of organization, although dissimilarity was greater among clades for the Bray–Curtis dendrogram compared to the Chao–Jaccard dendrogram. For example, the Chao–Jaccard method revealed that dissimilarity was highest at ~0.35, while the maximum dissimilarity for the Bray–Curtis method was ≤0.55 (Figure 6a,b). Only in the NAPF ecoregion were all eight of the functional algal groups found, which would explain the highest estimated functional richness S_{FX} and $S_{FXChao1}$ index values. Functional group taxa that distinguished this region included leathery macrophytes (fx grp. 5) and filamentous red algae (fx grp. 2.5). One of the most abundant and ubiquitous species belonging to algal fx. group 5 was *Fucus gardneri*, the primary cover forming alga on mussel assemblages throughout the Pacific Northwest. *F. gardneri* is a perennial brown seaweed that thrives in temperate, moist environments with a high level of resistance to grazing by herbivores and may completely dominate the mid intertidal zone, which is indicative of its low disturbance potential in the ecosystem (De Vogelaere & Foster, 1994; Steneck & Dethier, 1994). Of the algae representing functional group 2.5, *Pterosiphonia bipinnata* was the most abundant at sites within the NAPF and was significant in the nMDS analysis for differentiating this region at the functional group scale. *P. bipinnata* is the least resistant to grazing by *Littorina* spp. (Steneck & Watling, 1982) and standing stock of this alga were associated with caenogastropod and amphipod groups at most of the sites, which underscores its importance in the food web at the functional group-scale (Steneck & Dethier, 1994).

3.3 | The effect of wave exposure and substrate angle on mussel matrices

In all cases, the models that combined site and ecoregion as nested random effects provided the best AIC scores for explaining variation due to random effects. Shell length and matrix depth were found to be significantly smaller in wave-sheltered locations, while much of the variation in mussel shell length, matrix depth, and stratum index was explained by the combination of wave exposure and bench substrate (*L* [$\beta = 22.41$, Pr (>|t|) < .001], *MD* [$\beta = 26.87$, Pr (>|t|) < .001] and *SI* [$\beta = 2.70$, Pr(>|t|) = .02]), with both fixed and random effects (ecoregion and site, $R^2_{C\,(L)} = 0.82$, $R^2_{C\,(M)} = 0.45$ $R^2_{C\,(SI)} = 0.71$) explaining up to 90 times the variance in the models than the variance that

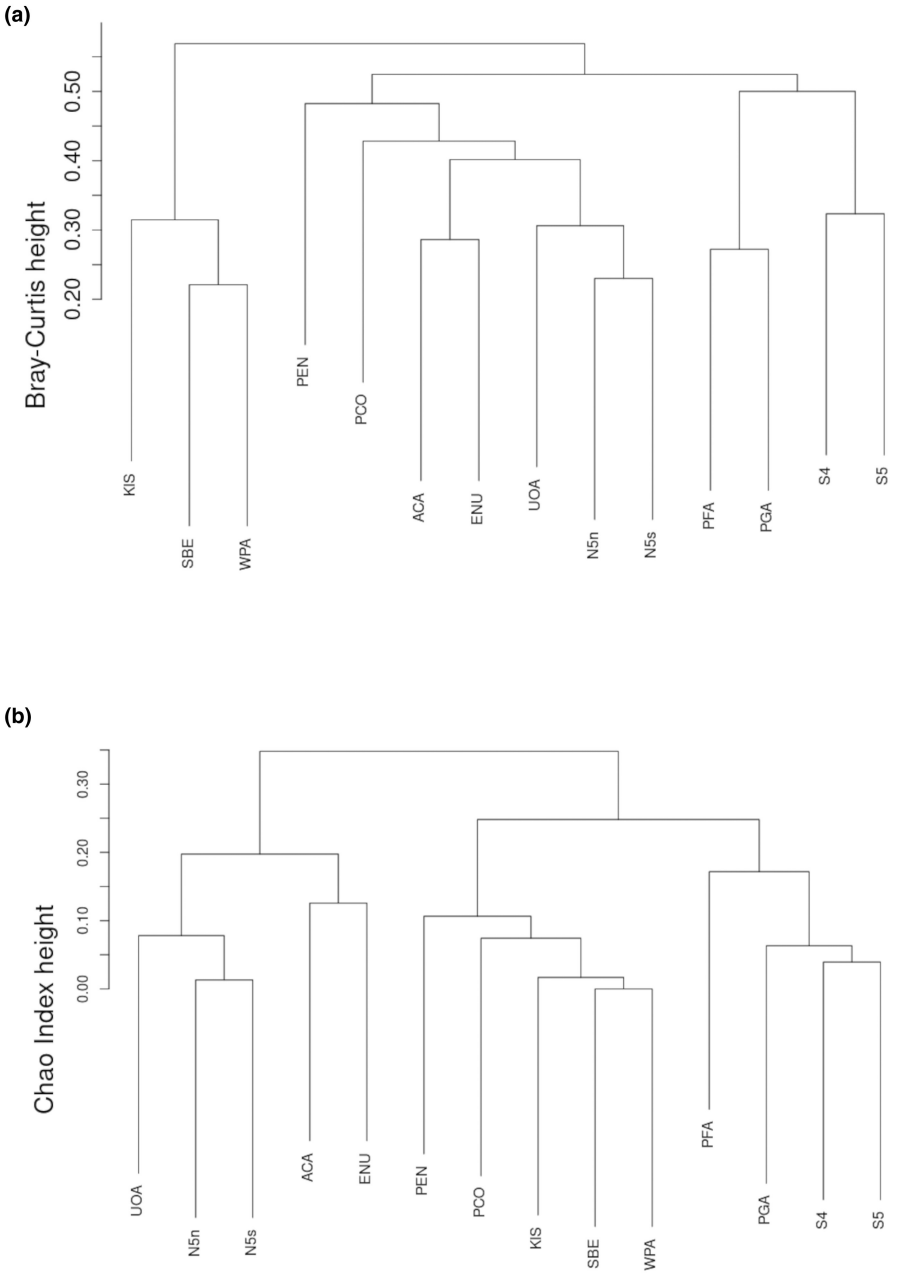

FIGURE 6 (a and b) Hierarchical dendrograms from Bray–Curtis measure of dissimilarity (top), and Chao–Jaccard dissimilarity (bottom) analyzed from the functional group data from all mussel plots from sites within all ecoregions. Bray–Curtis dissimilarity is a standard comparison of common species between two or more samples while Chao–Jaccard dissimilarity accounts for rare species when comparing two or more samples. The three-letter abbreviations for each site and mussel plot number are shown in each leaf of the cluster nodes: for the NAPF ecoregion, KIS = Kayak Island, SBE = Sage Beach, WPA = Whale Park, and PCO = Pirate's Cove; for the GUAY ecoregion, ACA = Playa Acapulco, ENU = El Nuro; for the Humboldtian ecoregion (HWS and HNS), PEN = Playa Ensenada, PFA = Playa Farallones, PEN = Playa Ensenada, PGA = Playa Gallardo, N5n, N5s, S4, and S5 = Reserva Punta San Juan.

was explained by the fixed effects alone ($R^2_{M\,(L)} = 0.08$, $R^2_{M\,(M)} = 0.04$ $R^2_{M\,(SI)} = 0.14$). The standard errors in the models for stratum index were lowest overall, which suggests that stratum index is the best predictor of complexity in mussel matrices (Table 4). The characteristically mono-layered mussel matrices (Guiñez & Castilla, 1999) sampled at Playa Acapulco were likely responsible for the higher standard errors in the models for shell length and matrix depth (the assemblages of *Brachidontes* sp. sampled at Playa Acapulco) were consistently mono-layered across all plots sampled, and the smaller shell sizes may be due to the age-class of the mussels (Torroglosa & Giménez, 2018). In other words, median shell lengths of the *Brachidontes* sp. assemblages at Acapulco were equal to the matrix depths of the assemblages, which skewed the data when fit with the shell length data from the other ecoregional groups. Although shell length is used in the formula to calculate stratum index, the calculation's formula includes measuring the area of substrate occupied by the mussel matrix as well as calculating a coefficient based on mussel size (Hosomi, 1985). The formula for the calculation of the stratum index of mussel matrices provides a standardized the dataset and in this case, the distribution of the residuals was relatively homogeneous with most of the variation in the model explained by the random effects (sites within ecoregional groups).

3.4 | Richness (I_{Mn}) and evenness (J) versus the nested variables

Differences in Menhinick's species richness (I_{Mn}) and Pielou's evenness (J) were tested with the Wilcoxen rank-sum test (Table 5) using the pooled data from all ecoregions and the nested explanatory

TABLE 4 Results from the linear mixed effects modeling of the dependent variables shell length ($n = 1095$), matrix depth ($n = 896$), and stratum index ($n = 86$) with wave exposure and substrate angle as the fixed effects and ecoregion and sites as the random effects.

	Shell length (L)					Matrix depth (M)					Stratum index (SI)				
Fixed effects	**Estimate**	**SE**	**Pr (>|t|)**	**R^2M, R^2C**	**F, Pr (>|f|)**	**Estimate**	**SE**	**Pr (>|t|)**	**R^2M, R^2C**	**F, Pr (>|f|)**	**Estimate**	**SE**	**Pr (>|t|)**	**R^2M, R^2C**	**F, Pr (>|f|)**
Exposed	22.41	3.92	**<0.001**	0.10, 0.84	44.62, **<0.001**	26.87	5.33	**<0.001**	0.03,0.45	5.40, **0.03**	2.70	0.54	**0.02**	0.004,0.65	0.26, 0.63
Sheltered	−7.28	1.09	**<0.001**			−7.36	3.17	**0.02**			−0.19	0.38	0.63		
Bench	19.02	4.56	**<0.001**	0.004, 0.83	1.23, 0.27	24.38	5.99	**<0.001**	0.001, 0.43	0.07, 0.80	2.45	0.59	**0.01**	0.014,0.65	0.65, 0.43
Vertical	1.24	1.12	0.27			−0.87	3.36	0.80			0.34	0.42	0.43		
Exposed*bench	20.91	3.89	**<0.001**	0.08, 0.82	15.83, **<0.001**	26.91	5.38	**<0.001**	0.04, 0.45	0.07	2.73	0.43	**<0.001**	0.14, 0.71	2.57, 0.09
Exposed*vertical	2.01	1.31	0.13			1.24	4.24	0.77		0.07	1.01	0.61	0.11		
Sheltered*bench	1.93	5.13	0.71			2.11	9.91	0.83		0.59	−0.11	1.25	0.11		
Sheltered *vertical	−5.46	1.64	**0.001**			−8.43	4.85	0.08		0.07	−0.63	0.66	0.35		

Note: Marginal coefficients of determination for fixed effects (R^2M) and conditional coefficient of determination for fixed and random effects (R^2C) were calculated for each model. *F*-statistics from analysis of variance with significance at Pr(|f|) < .05.

variables mono-layered matrices with cover versus mono-layered matrices without cover, and multi-layered matrices with cover versus mono-layered matrices without cover (Table 5). Multi-layered matrices defined by stratum index and matrix depth were significantly higher for I_{Mn}, with the greatest variances in median values found between multi-layered canopied matrices and mono-layered matrices without cover (SI $|M_1 - M_2| = 1.22$, $p < .001$; MD $|M_1 - M_2| = 1.09$, $p < .001$) (Figure 7). Rankings for all but one of the pairwise comparisons (mono-layered canopied matrices versus multi-layered matrices without cover as defined by SI) were significant for differences in median I_{Mn} ($p < .05$) for matrices defined both by SI and MD. Post hoc analysis of variance was performed on pooled canopied matrices ($n = 44$) versus pooled matrices without cover ($n = 42$) for both stratum index and matrix depth; for a large effect size ($d = 0.40$, $n = 86$) the power of the analysis $1-\beta = 0.96$ (Cohen, 1988). Mean Menhinick's richness (D) was 1.5 times greater for canopied matrices ($F = 38.99$, $Pr(>F) < .001$) compared to (D) in matrices without cover, regardless of the complexity of the matrix.

Variations in median Pielou's evenness J were generally much smaller than the variations found for I_{mn}. Only one of the pairwise comparisons (mono-layered matrices versus mono-layered matrices without cover) was significant for differences in median J, although the variation was quite small (SI $|M_1 - M_2| = 0.08$, $p = .04$). There were no significant differences in the medians of I_{mn} and J when the methods for defining mussel matrices SI and MD were compared according to each respective level of mussel layering and the presence or absence of an algal cover.

4 | DISCUSSION

4.1 | Mussel layers, algal cover, and variations in species richness and evenness

In this study, we demonstrate the value of macroalgal cover in driving patterns of macrofaunal diversity intertidal rocky systems, from the northern to the southern Pacific, specifically, algal cover and the interaction between wave-exposure and bench type substrate were the strongest factors shaping intertidal communities. The structure of mussel assemblages at wave-exposed sites showed more complexity than did mussel assemblages at wave-sheltered locations, algal cover was significantly associated with higher levels of species richness regardless of the complexity of the matrix, while canopied multi-layered matrices were highest in species richness and accounted for the highest variance in species richness index when compared to mono-layered matrices with no algal cover. The relationship between stratum index and species richness was stronger than the relationship between species richness and matrix depth, therefore we suggest that the stratum index of a mussel matrix is a better predictor of species richness. In general, mono-layered matrices had significantly lower indices of species evenness than did multi-layered matrices, in a very similar manner to Prado and Castilla (2006). Furthermore, there was no significant difference

TABLE 5 Results from the Wilcoxen rank-sum test for comparison of the medians for Menhinick's species richness (SMN) and Pielou's evenness (J) in mussel matrices defined by the stratum index, left column (mono-layered matrices with algal cover [$n = 11$], mono-layered matrices without cover [$n = 11$], multi-layered matrices with cover [$n = 33$], multi-layered matrices without cover [$n = 31$]) and matrices defined by depth, right column (mono-layered matrices with algal cover [$n = 16$], mono-layered matrices without cover [$n = 16$], multi-layered matrices with cover [$n = 30$], multi-layered matrices without cover [$n = 27$]).

	Menhinick's species richness (IMn)-stratum index						Menhinick's species richness (IMm)-matrix depth					
	|M1 − M2|	CI (2.5 pctl)	CI (98 pctl)	CI (bootstrapped 2.5 pctl)	CI (bootstrapped 98 pctl)	*p*-Value	|M1 − M2|	CI (2.5 pctl)	CI (98 pctl)	CI (bootstrapped 2.5 pctl)	CI (bootstrapped 98 pctl)	*p*-Value
Multi-layer with canopy v. mono-layer with canopy	0.35	−0.08	−0.47	−0.02	−0.44	**.02**	0.29	−0.1	−0.46	−0.16	−0.42	**<.001**
Mono-layer with canopy v. mono-layer no canopy	0.87	0.67	0.99	1.14	1.41	**<.001**	0.8	0.39	0.97	0.67	1.03	**<.001**
Mono-layer with canopy v. multi-layer no canopy	0.18	0.01	0.04	−0.03	0.38	.05	0.27	0.03	0.44	0.06	0.46	**.03**
Multi-layer with canopy v. mono-layer without canopy	1.22	−1.3	−0.97	−1.04	−1.36	**<.001**	1.09	−1.24	−0.69	0.06	0.46	**<.001**
Multi-layer with canopy v. multi-layer no canopy	0.53	0.31	0.65	0.27	0.61	**<.001**	0.56	0.28	0.7	0.39	0.71	**<.001**
Mono-layer without canopy v. multi-layer without canopy	0.69	−4.3	−0.85	−0.45	−0.87	**<.001**	0.53	−0.69	−0.22	−0.82	−0.09	**.01**
	Pielou's evennes (J) stratum index						**Pielou's evenness (J) matrix depth**					
	|M1 − M2|	CI (2.5 pctl)	CI (98 pctl)	CI (bootstrapped 2.5 pctl)	CI (bootstrapped 98 pctl)	*p*-Value	|M1 − M2|	CI (2.5 pctl)	CI (98 pctl)	CI (bootstrapped 2.5 pctl)	CI (bootstrapped 98 pctl)	*p*-Value
Multi-layer with canopy v. mono-layer with canopy	0.04	−0.08	0.04	−0.09	0.05	.45	0.41	−0.05	0.06	−0.07	0.07	.97
Mono-layer with canopy v. mono-layer without canopy	0.08	−0.13	$8.63e^{-5}$	−0.13	0.04	.06	0	−0.08	0.03	−0.1	0.05	.38
Mono-layer with canopy v. multi-layer without canopy	0.45	−0.05	0.07	−0.06	0.08	0.59	0.06	−0.02	0.10	−0.02	0.12	.15
Multi-layer with canopy v. mono-layer without canopy	0.04	−0.02	0.09	−0.04	0.08	.28	0.04	−0.02	0.08	−0.02	0.08	.29
Multi-layer with canopy v. multi-layer without canopy	0.59	$4.09e^{-5}$	$7.0e^{-2}$	−0.02	0.08	.08	0.03	−0.01	0.08	−0.01	0.09	.10
Mono-layer without canopy v. multi-layer without canopy	0.09	0.02	0.14	0	0.11	**.02**	0.06	0.02	0.12	0.02	0.12	**.01**

Note: Confidence intervals from from the bootstrapped data (10^4 re-samples) for the test are within 2.5 and 98 percentiles. Absolute values of the difference in medians |M1 − M2 | and significance of test at $p < .05$.

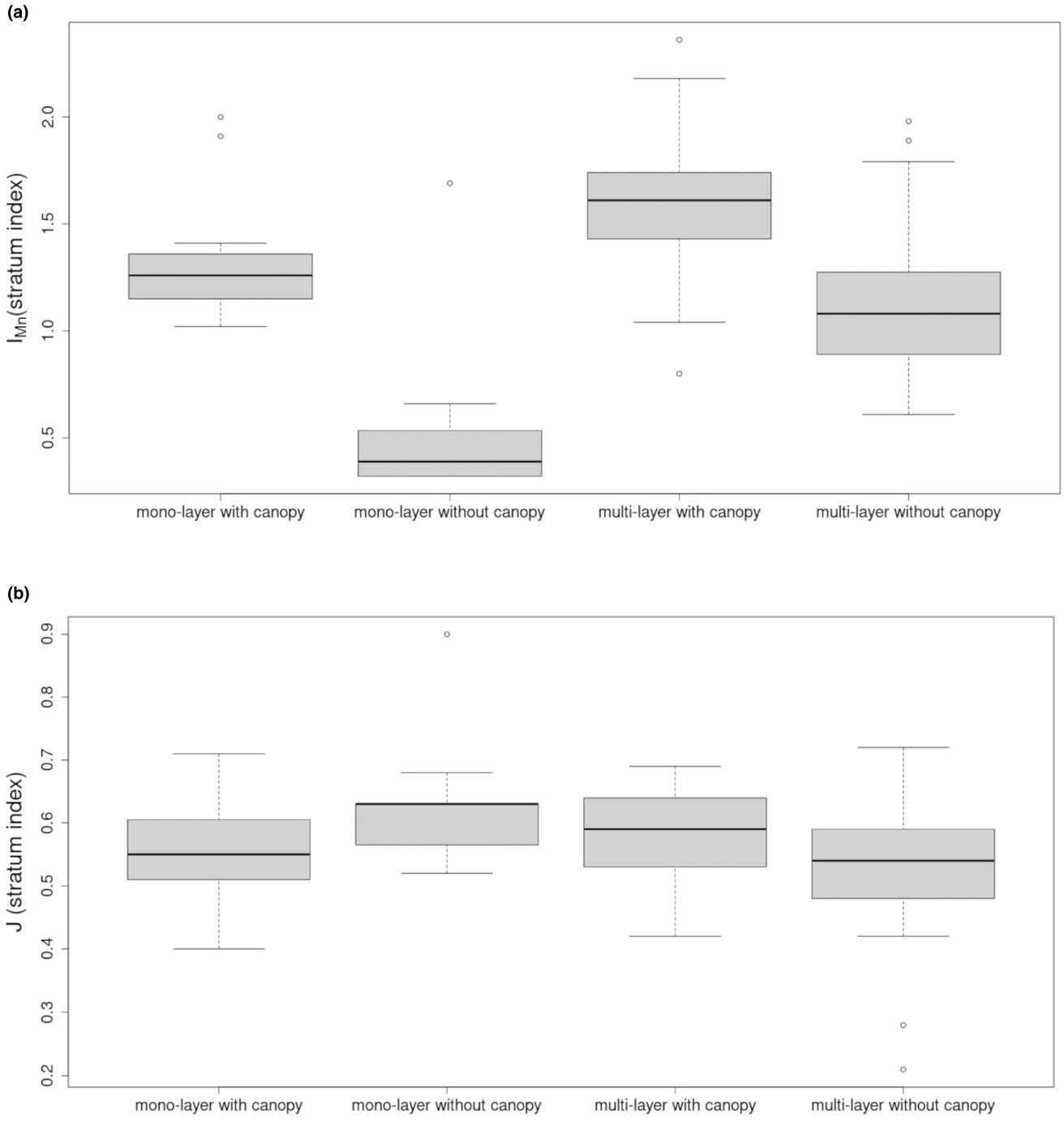

FIGURE 7 Five number summary box plots depicting Menhinick's species richness (IMn) and Pielou's evenness (J) in mussel matrices defined by stratum index or matrix depth with or without algal canopies. (a) IMn in matrices by stratum index, (b) J in matrices by matrix depth, (c) IMn in matrices by stratum index, (d) J in matrices by matrix depth.

between the presence of an algal cover and the level of species evenness in the mussel assemblages sampled on the broad ecoregional scale that our samples were based on.

There is an underlying factor differentiating species richness and evenness between mussel communities in the HWS ecoregion and the HNS ecoregion. The removal of an apex predator has the potential to cause changes in trophic hierarchies (Castilla & Durán, 1985; Moreno et al., 1986), and the abundances of *P. purpuratus* at Playa Ensenada and Playa Farallones may have been linked to the unregulated harvesting of mussel predators that was observed during each field season. The asteroid *Heliaster helianthus* was present to some degree at UOA and was abundant at PSJ in the HNS ecoregion, was observed foraging on stands of *P. purpuratus*, but was not seen at any of the sites within the HWS ecoregion (Wilbur, in review). *Concholepas concholepas* (locally known as "loco"), a slow-growing carnivorous muricid snail ranging from 5 to 7 cm in length, was also seen foraging on mussels in the high to mid-intertidal zone at PSJ. The objective when selecting our study sites was to sample

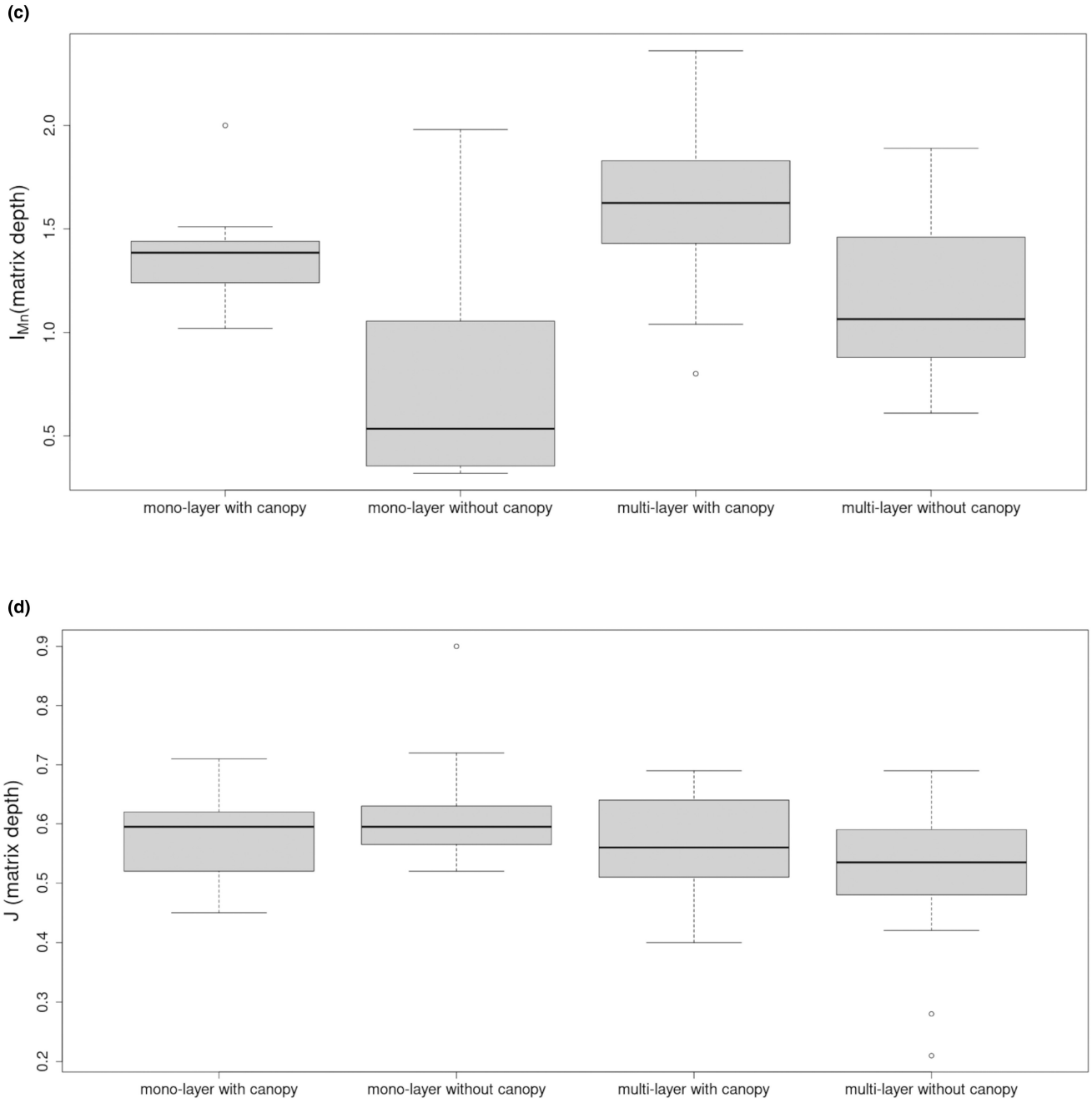

FIGURE 7 (Continued)

from areas of limited or low human impact, however, there was some level of human activity at all of the sites and PSJ was no exception. The waters surrounding PSJ have been historically subject to illegal fishing pressure (divers could be seen using hookah to fish for invertebrates only meters from shore) and thus the exists potential to drastically change species richness and trophic structures in the intertidal communities at PSJ (Harley & Rogers-Bennett, 2004; Kunze et al., 2021; Steneck et al., 2004). Nevertheless, PSJ provided a unique opportunity to survey mussel assemblages in a nearly pristine environment, and we suggest that the *P. purpuratus* assemblages at PSJ possess a trophic structure distinct from the *P. purpuratus* assemblages at the sites at UOA and within the HWS ecoregion.

4.2 | Biodiversity patterns

Mussels from assemblages sampled throughout all ecoregional groups shared a similar characteristic of hosting sessile epibionts such as barnacles and algal sporelings on their shells. Of significance was the presence of species that were rare and unique in the quadrats such as the motile actinids *Metridium senile* in the NAPF ecoregion and *Phymactis clematis* in the HWS ecoregion. Species typically found as later-stage adults in the lower intertidal or subtidal zones may recruit in higher zones during larval or early life stages, which is an advantageous strategy in terms of benefiting from the filter-feeding strategy of the mussels as well as avoiding competition with

conspecifics as well as other species (Caro et al., 2010; Dahlhoff & Menge, 1996).

Steneck et al. (2004) have suggested that fishing pressure can cause an effect of trophic cascades in marine environments, with species from one functional trophic group replacing species from an existing group. It has been established historically that the removal of a top predator has the potential to cause trophic level shifts and significant changes to the food web in localized ecosystems (Paine, 1966; Steneck et al., 2004; Whittaker, 1972). As mentioned previously, we observed an active artisanal fishing effort for "loco" during the surveys in the HWS ecoregion. This fishery required breath-hold divers in heavy surf to hand pick "loco" from rocky substrate. At sites within the HWS, we observed fishermen returning to the beach with large pouches full of "loco" and discarding the shucked shells in the supratidal zone. The only sites where living *C. concholepas* were counted during our surveys were at sites inside the marine protected reserve at PSJ where fishing of any kind is prohibited, but as mentioned previously, illegal fishing does occur on occasion. *C. concholepas* has a wide regional distribution and vertical distribution and because of its prolonged epineustonic phase, the dispersal potential for this species is considerable (Cárdenas et al., 2015; DiSalvo, 1988). There is strong evidence to suggest that *C. concholepas* plays a role as a keystone species in the southeast Pacific intertidal zone and while it is highly likely that a population of *C. concholepas* may be beyond reach of the fishermen in unregulated areas of the Peruvian coast.

The structural patterns for mussel communities at the algal and invertebrate functional group level in the warm temperate region of Peru and the cold temperate region of Alaska were very similar. This pattern has also been observed in the past in micro-biome communities associated with brown algae that show similar structure across different ecoregions (Capistrant-Fossa et al., 2021). Functional group turnover (beta diversity) was pronounced among ecoregional-groups, with significant overlap among most sites within each group. The greatest Bray–Curtis distance between two sites occurred between ACA and ENU in the GUAY ecoregion, likely due to the low number of species found in the mussel communities at ACA. The relatively low richness indices and the characteristically mono-layered matrices at ACA lend further evidence to our hypothesis that shell length can be used as a predictor of species richness in mussel communities (Wilbur et al., 2023).

4.3 | The effect of wave exposure and substrate angle on mussel matrices

Prado and Castilla (2006) found that matrix depth had a significant effect on species evenness in assemblages of *P. purpuratus* on a very localized scale, with stratified matrices having significantly lower species evenness. The results of this study are consistent with the results of local scale research done by Prado and Castilla (2006) in mussel assemblages at Punta de Tralca in Chile, and our findings show that algal cover and mussel stratification can be used to predict species diversity and evenness in macro-scale communities associated with mussel assemblages throughout several marine ecoregions. Additionally, our results in relation to the effect of wave exposure on the homogeneity of mussel stratification are supported by Dahlhoff and Menge's (1996) findings that mussel physiology and growth are variable according to distinct environmental factors that drive food availability, as this too was consistent across mussel species on a broad regional scale. In summary, this study constitutes the first effort made to assess species diversity, compare functional group diversity, and measure the effects of biological and environmental factors on mussel assemblages and associated macro-communities using regionally distinct mussel species across a broad eco-regional scale. This is also the first effort to research macro-invertebrate and algal communities at previously unresearched areas of the Peruvian and Alaskan coasts, including a protected marine area in the south of Peru.

ACKNOWLEDGMENTS

Appreciations are due to Susana Cárdenas Alayza at the Center for Environmental Sustainability of Universidad de Cayetano Heredia in Lima Peru and the staff members of the Reserva Punta San Juan in Marcona Peru for their assistance with permitting and fieldwork, to Bruno Ibanez-Erquiaga at the Laboratorio de Ciencias del Mar, Universidad de Cayetano Heredia for his invaluable assistance with field guides and logistics, to the Ministero de la Producción de Peru for the permit to collect marine specimens, the Servicio Nacional de Áreas Naturales for permission to work in the Reserve, Shaleyla Kalez of EcoOceanica for her assistance with logistics in the northernmost ecoregion of Peru, and Prof. Aldo Pacheco from the Universidad de Cayetano for his assistance with logistics and species identification in Antofagasta Chile. This study was partially supported by the University of Aberdeen, School of Biological Sciences. We would also like to thank the MASTS pooling initiative and contributing institutions. The authors report no conflict of interest. Data is available upon request.

FUNDING INFORMATION

The Marine Alliance for Science and Technology for Scotland). MASTS is funded by the Scottish Funding Council (grant reference HR09011).

DATA AVAILABILITY STATEMENT

Data available upon request.

ORCID

Vasilis Louca https://orcid.org/0000-0001-9560-0479

REFERENCES

Akaike, H. (1974). A new look at the statistical model identification. *IEEE Transactions on Automatic Control*, *19*, 716–723.

Altieri, A. H., Silliman, B. R., & Bertness, M. D. (2007). Hierarchical organization via a facilitation cascade in intertidal cordgrass bed communities. *The American Naturalist*, *169*(2), 195–206. https://doi.org/10.1086/510603

Alvarado, J. L., & Castilla, J. C. (1996). Tridimensional matrices of mussels Perumytilus purpuratus on intertidal platforms with varying wave forces in Central Chile. *Marine Ecology Progress Series*, *133*, 135–141.

Arakaki, N., Carbajal, P., Gamarra, A., Gil-Kodaka, P., & Ramírez, M. (2019). *Macroalgas de la costa*. Central del Perú.

Arakaki, N., Carbajal, P., Gamarra, A., Gil-Kodaka, P., & Ramirez, M. E. (2018). *Macroalgas de pucusana guia de campo* (Vol. *56*). Universidad Nacional Agraria La Molina.

Benedetti-Cecchi, L., Nuti, S., & Cinelli, F. (1996). Analysis of spatial and temporal variability in interactions among algae, limpets and mussels in low-shore habitats on the west coast of Italy. *Marine Ecology Progress Series*, *144*, 87–96.

Blanchette, C. A., Wieters, E. A., Broitman, B. R., Kinlan, B. P., & Schiel, D. R. (2009). Trophic structure and diversity in rocky intertidal upwelling ecosystems: A comparison of community patterns across California, Chile, South Africa and New Zealand. *Progress in Oceanography*, *83*(1), 107–116. https://doi.org/10.1016/j.pocean.2009.07.038

Bousfield, E. L., & Hendrycks, E. A. (1995). The amphipod family Pleustidae on the Pacific coast of North America. Part III. Subfamilies Parapleustinae, Dactylopleustinae and Pleusirinae: Systematics and distributional ecology. *Amphipacifica*, *2*, 65–133.

Bray, J. R., & Curtis, J. T. (1957). An ordination of the upland forest communities of southern Wisconsin. *Ecological Monographs*, *27*, 326–349.

Bryson, E. S., Trussell, G. C., & Ewanchuk, P. J. (2014). Broad-scale geographic variation in the organization of rocky intertidal communities in the Gulf of Maine. *Ecological Monographs*, *84*, 579–597.

Bulleri, F., Benedetti-Cecchi, L., Acunto, S., Cinelli, F., & Hawkins, S. J. (2002). The influence of canopy algae on vertical patterns of distribution of low-shore assemblages on rocky coasts in the Northwest Mediterranean. *Journal of Experimental Marine Biology and Ecology*, *267*, 89–106.

Burger, J., Gochfeld, M., & Jewett, S. (2006). Selecting species for marine assessment of radionuclides around Amchitka: Planning for diverse goals and interests. *Environmental Monitoring and Assessment*, *123*, 371–391.

Burnham, K. P., Anderson, D. R., & Huyvaert, K. P. (2011). AIC model selection and multimodel inference in behavioral ecology: Some background, observations, and comparisons. *Behavioral Ecology and Sociobiology*, *65*, 23–35.

Buschbaum, C., Dittmann, S., Hong, J.-S., Hwang, I.-S., Strasser, M., Thiel, M., Valdivia, N., Yoon, S. P., & Reise, K. (2009). Mytilid mussels: Global habitat engineers in coastal sediments. *Helgoland Marine Research*, *63*, 47–58.

Capistrant-Fossa, K. A., Morrison, H. G., Engelen, A. H., Quigley, C. T., Morozov, A., Serrão, E. A., Brodie, J., Gachon, C. M. M., Badis, Y., Johnson, L. E., Hoarau, G., Abreu, M. H., Tester, P. A., Stearns, L. A., & Brawley, S. H. (2021). The microbiome of the habitat-forming brown alga Fucus vesiculosus (Phaeophyceae) has similar cross-Atlantic structure that reflects past and present drivers1. *Journal of Phycology*, *57*, 1681–1698.

Cárdenas, L., Castilla, J. C., & Viard, F. (2015). Hierarchical analysis of the population genetic structure in *Concholepas concholepas*, a marine mollusk with a long-lived dispersive larva. *Marine Ecology*, *37*, 359–369. https://doi.org/10.1111/maec.12286

Caro, A. U., Navarrete, S. A., & Castilla, J. C. (2010). Ecological convergence in a rocky intertidal shore metacommunity despite high spatial variability in recruitment regimes. *Proceedings of the National Academy of Sciences of the United States of America*, *107*, 18528–18532.

Castilla, J. C., & Durán, L. R. (1985). Human exclusion from the rocky intertidal zone of Central Chile: The effects on Concholepas Concholepas (Gastropoda). *Oikos*, *45*, 391–399.

Chao, A. (1984). Nonparametric estimation of the number of classes in a population. *Scandinavian Journal of Statistics*, *11*, 265–270.

Chao, A. (1987). Estimating the population size for capture-recapture data with unequal catchability. *Biometrics*, *43*, 783–791.

Chao, A., Chazdon, R. L., Colwell, R. K., & Shen, T.-J. (2005). A new statistical approach for assessing similarity of species composition with incidence and abundance data. *Ecology Letters*, *8*, 148–159.

Chao, A., Gotelli, N. J., Hsieh, T. C., Sander, E. L., Ma, K. H., Colwell, R. K., & Ellison, A. M. (2014). Rarefaction and extrapolation with hill numbers: A framework for sampling and estimation in species diversity studies. *Ecological Monographs*, *84*(1), 45–67.

Cohen, J. (1988). Set correlation and contingency tables. *Applied Psychological Measurement*, *12*(4), 425–434.

Colwell, R., & Coddington, J. (1994). Estimating terrestrial biodiversity through extrapolation. *Philosophical Transactions of the Royal Society of London. Series B, Biological Sciences*, *345*, 101–118.

Colwell, R. K. (2013). Estimates: Statistical estimation of species richness and shared species from samples. Version 9. – User's Guide and application at http://purl.oclc.org/estimates

Colwell, R. K., Chao, A., Gotelli, N. J., Lin, S.-Y., Mao, C. X., Chazdon, R. L., & Longino, J. T. (2012). Models and estimators linking individual-based and sample-based rarefaction, extrapolation and comparison of assemblages. *Journal of Plant Ecology*, *5*, 3–21.

Colwell, R. K., & Elsensohn, J. E. (2014). EstimateS turns 20: Statistical estimation of species richness and shared species from samples, with non-parametric extrapolation. *Ecography*, *37*, 609–613.

Colwell, R. K., Mao, C. X., & Chang, J. (2004). Interpolating, extrapolating, and comparing incidence-based species accumulation curves. *Ecology*, *85*, 2717–2727.

Connell, J. H. (1961). The influence of interspecific competition and other factors on the distribution of the barnacle Chthamalus Stellatus. *Ecology*, *42*, 710–723.

Connolly, S. R., & Roughgarden, J. (1999). Theory of marine communities: Competition, predation, and recruitment-dependent interaction strength. *Ecological Monographs*, *69*, 277–296.

Dahlhoff, E. P., & Menge, B. A. (1996). Influence of phytoplankton concentration and wave exposure on the ecophysiology of *Mytilus californianus*. *Marine Ecology Progress Series*, *144*, 97–107.

D'Antonio, C. M. (1986). Role of sand in the domination of hard substrata by the intertidal alga *Rhodomela larix*. *Marine Ecology Progress Series*, *27*, 263–275.

Dawson, Y. E., Acleto, C., & Foldvik, N. (1964). *The seaweeds of Peru* (p. 111). Weinheim Verlag Von J. Cramer.

Dayrat, B., Goulding, T. C., & White, T. R. (2014). Diversity of indo-West Pacific Siphonaria (Mollusca: Gastropoda: Euthyneura). *Zootaxa*, *3779*, 246–276.

De Vogelaere, A. P., & Foster, M. S. (1994). Damage and recovery in intertidal *Fucus gardneri* assemblages following the Exxon Valdez oil spill. *Marine Ecology Progress Series. Oldendorf*, *106*, 263–271.

DiSalvo, L. H. (1988). Observations on the larval and post-metamorphic life of *Concholepas concholepas* (Bruguiére 1789) in laboratory culture. *The Veliger*, *30*(4), 358–368.

Engle, J. M. (2008). *Unified monitoring protocols for the multi-agency rocky intertidal network*. Marine Science Institute, University of California.

Firstater, F. N., Hidalgo, F. J., Lomovasky, B. J., Ramos, E., Gamero, P., & Iribarne, O. O. (2011). Habitat structure is more important than nutrient supply in modifying mussel bed assemblage in an upwelling area of the Peruvian coast. *Helgoland Marine Research*, *65*, 187–196.

Fisher, R. A., Corbett, A. S., & Williams, C. B. (1943). The relationship between the number of species and the number of individuals in a random sample of an animal population. *Journal of Animal Ecology*, *12*, 42–58.

Frechette, M., Aitken, A. E., & Page, L. (1992). Interdependence of food and space limitation of a benthic suspension feeder: Consequences for self-thinning relationships. *Marine Ecology Progress Series. Oldendorf*, *83*, 55–62.

Guiñez, R., & Castilla, J. C. (1999). A tridimensional self-thinning model for multilayered intertidal mussels. *The American Naturalist*, *154*, 341–357.

Güller, M., Zelaya, D. G., & Ituarte, C. (2016). How many Siphonaria species (Gastropoda: Euthyneura) live in southern South America? *Journal of Molluscan Studies*, *82*, 80–96.

Harley, C. D., & Helmuth, B. S. (2003). Local-and regional-scale effects of wave exposure, thermal stress, and absolute versus effective shore level on patterns of intertidal zonation. *Limnology and Oceanography*, *48*, 1498–1508.

Harley, C. D. G., & Rogers-Bennett, L. (2004). *The potential synergistic effects of climate change and fishing pressure on exploited invertebrates on rocky intertidal shores*. Effects of Climate Change and fishing pressure on exploited invertebrates CalCOFI No. 45.

Helmuth, B., Broitman, B. R., Blanchette, C. A., Gilman, S., Halpin, P., Harley, C. D., O'Donnell, M. J., Hofmann, G. E., Menge, B., & Strickland, D. (2006). Mosaic patterns of thermal stress in the rocky intertidal zone: Implications for climate change. *Ecological Monographs*, *76*, 461–479.

Helmuth, B. S. (1998). Intertidal mussel microclimates: Predicting the body temperature of a sessile invertebrate. *Ecological Monographs*, *68*, 51–74.

Hosomi, A. (1985). On the persistent trend of constant biomass and the constant total occupation area of the mussel *Mytilus galloprovincialis* (Lamarck). *Venus (Japanese Journal of Malacology)*, *44*, 33–48.

Hosomi, A. (1987). On the density effect in populations of the mussel, *Mytilus galloprovincialis*. *Venus (Japanese Journal of Malacology)*, *46*, 116–126.

Howe, M. A. (1914). *Marine algae of Peru* (p. 330). Press of the New era Print. Co.

Hubbell, S. P. (2015). Estimating the global number of tropical tree species, and Fisher's paradox. *Proceedings of the National Academy of Sciences of the United States of America*, *112*, 7343–7344.

Ibanez-Erquiaga, B., Pacheco, A. S., Rivadeneira, M. M., & Tejada, C. L. (2018). Biogeographical zonation of rocky intertidal communities along the coast of Peru (3.5–13.5° S Southeast Pacific). *PLoS One*, *13*, e0208244.

Jenkins, S. R., Hawkins, S. J., & Norton, T. A. (1999). Direct and indirect effects of a macroalgal canopy and limpet grazing in structuring a sheltered inter-tidal community. *Marine Ecology Progress Series*, *188*, 81–92.

Konar, B., Iken, K., Cruz-Motta, J. J., Benedetti-Cecchi, L., Knowlton, A., Pohle, G., Miloslavich, P., Edwards, M., Trott, T., Kimani, E., Riosmena-Rodriguez, R., Wong, M., Jenkins, S., Silva, A., Pinto, I. S., & Shirayama, Y. (2010). Current patterns of macroalgal diversity and biomass in northern hemisphere rocky shores. *PLoS One*, *5*, e13195.

Kozloff, E. (1996). *Marine invertebrates of the Pacific northwest with additions and corrections* (p. 552). University of Washington Press.

Kunze, C., Wölfelschneider, M., & Rölfer, L. (2021). Multiple driver impacts on rocky intertidal systems: The need for an integrated approach. *Frontiers in Marine Science*, *8*, 667168.

Kuznetsova, A., Brockhoff, P. B., & Christensen, R. H. B. (2017). lmerTest package: Tests in linear mixed effects models. *Journal of Statistical Software*, *82*, 1–26.

Leite, F. P., Bottcher, C., Lewinsohn, I. D., Siqueira, S. G., Mansur, K. F., Longo, P. A., & Vieira, E. A. (2021). Asymmetric effects of changes in the habitat-forming algae Sargassum on different associated mobile faunas along São Paulo coast, Brazil. *Marine Ecology*, *42*(3), e12649.

Leonard, G. H. (1999). Positive and negative effects of intertidal algal canopies on recruitment and survival of barnacles. *Marine Ecology Progress Series*, *178*, 241–249.

Magnussen, S., & Boyle, T. J. B. (1995). Estimating sample size for inference about the Shannon-Weaver and the Simpson indices of species diversity. *Forest Ecology and Management*, *78*, 71–84.

McDonald, J. H., Seed, R., & Koehn, R. K. (1991). Allozymes and morphometric characters of three species of Mytilus in the northern and southern hemispheres. *Marine Biology*, *111*, 323–333.

Mendez, L. T. (2002). *Guia de biodiversidad* (p. 63). Departamento de Acuicultura Facultad de Recursos del Mar Universidad de Antofagasta.

Menge, B. A. (1992). Community regulation: Under what conditions are bottom-up factors important on rocky shores? *Ecology*, *73*, 755–765.

Menge, B. A., Daley, B. A., Wheeler, P. A., Dahlhoff, E., Sanford, E., & Strub, P. T. (1997). Benthic–pelagic links and rocky intertidal communities: Bottom-up effects on top-down control? *Proceedings of the National Academy of Sciences of the United States of America*, *94*, 14530–14535.

Menge, B. A., Daley, B. A., Wheeler, P. A., & Strub, P. T. (1997). Rocky intertidal oceanography: An association between community structure and nearshore phytoplankton concentration. *Limnology and Oceanography*, *42*, 57–66.

Menge, B. A., Sanford, E., Daley, B. A., Freidenburg, T. L., Hudson, G., & Lubchenco, J. (2002). Inter-hemispheric comparison of bottom-up effects on community structure: Insights revealed using the comparative-experimental approach. *Ecological Research*, *17*, 1–16.

Menhinick, E. F. (1964). A comparison of some species-individuals diversity indices applied to samples of field insects. *Ecology*, *45*, 859–861.

Moreno, C. A., Lunecke, K. M., & Lépez, M. I. (1986). The response of an intertidal Concholepas concholepas (Gastropoda) population to protection from man in southern Chile and the effects on benthic sessile assemblages. *Oikos*, *46*, 359–364.

Oksanen, J., Blanchet, F. G., Friendly, M., Kindt, R., Legendre, P., McGlinn, D., Minchin, P. R., O'Hara, R. B., Simpson, G., Solymos, P., Stevens, M. H. H., Szöcs, E., & Wagner, H. (2020). *Vegan: Community Ecology Package. R Package Version 2.5-7*. https://cran.r-project.org/web/packages/vegan/index.html

Okuda, T., Noda, T., Yamamoto, T., Ito, N., & Nakaoka, M. (2004). Latitudinal gradient of species diversity: Multi-scale variability in rocky intertidal sessile assemblages along the northwestern Pacific coast. *Population Ecology*, *46*, 159–170.

Paine, R. T. (1966). Food web complexity and species diversity. *The American Naturalist*, *100*, 65–75.

Peake, A. J., & Quinn, G. P. (1993). Temporal variation in species-area curves for invertebrates in clumps of an intertidal mussel. *Ecography*, *16*, 269–277.

Pielou, E. C. (1966). The measurement of diversity in different types of biological collections. *Journal of Theoretical Biology*, *13*, 131–144.

Prado, L., & Castilla, J. C. (2006). The bioengineer Perumytilus purpuratus (Mollusca: Bivalvia) in Central Chile: Biodiversity, habitat structural complexity and environmental heterogeneity. *Journal of the Marine Biological Association of the United Kingdom*, *86*, 417–421.

R Core Team. (2020). *R: A language and environment for statistical computing*. R Foundation for Statistical Computing.

Rabinowitz, G. B. (1975). An introduction to nonmetric multidimensional scaling. *American Journal of Political Science*, *19*, 343–390.

Romero, O. Z. (2002). *Guia de biodiversidad* (p. 70). Departamento de Acuicultura Facultad de Recursos del Mar Universidad de Antofagasta.

RStudio Team. (2020). *RStudio: Integrated development environment for R. 1.3.1093*. RStudio, PBC.

Schonbeck, M. W., & Norton, T. A. (1979). Drought-hardening in the upper-shore seaweeds *Fucus spiralis* and *Pelvetia canaliculata*. *Journal of Ecology*, *67*, 687–696.

Shannon, C. E. (1948). A mathematical theory of communication. *The Bell System Technical Journal*, *27*, 379–423.

Siegel, S. (1957). Nonparametric statistics. *The American Statistician*, *11*, 13–19.

Simpson, E. H. (1949). Measurement of diversity. *Nature*, *163*, 688.

Spalding, M. D., Fox, H. E., Allen, G. R., Davidson, N., Ferdaña, Z. A., Finlayson, M., Halpern, B. S., Jorge, M. A., Lombana, A., Lourie, S. A., Martin, K. D., McManus, E., Molnar, J., Recchia, C. A., & Robertson,

J. (2007). Marine ecoregions of the world: A bioregionalization of coastal and shelf areas. *Bioscience*, *57*, 573–583.
Stachowicz, J. J., Graham, M., Bracken, M. E., & Szoboszlai, A. I. (2008). Diversity enhances cover and stability of seaweed assemblages: The role of heterogeneity and time. *Ecology*, *89*, 3008–3019.
Steneck, R. S. (1988). Herbivory on coral reefs: A synthesis. In *Proc. 6 th Int. Coral Reef Symp.*, *1988* (Vol. *1*, pp. 37–49).
Steneck, R. S., & Dethier, M. N. (1994). A functional group approach to the structure of algal-dominated communities. *Oikos*, *69*, 476–498.
Steneck, R. S., Vavrinec, J., & Leland, A. V. (2004). Accelerating trophic-level dysfunction in kelp forest ecosystems of the western North Atlantic. *Ecosystems*, *7*, 323–332.
Steneck, R. S., & Watling, L. (1982). Feeding capabilities and limitation of herbivorous molluscs: A functional group approach. *Marine Biology*, *68*, 299–319.
Storero, L. P., Avaca, M. S., & Roche, A. (2022). Living under Ulva canopy: The case of the scavenger snail Buccinastrum deforme in a eutrophic macrotidal bay in Patagonia (Argentina). *Marine Ecology*, *43*(4), e12718.
Strong, W. L. (2016). Biased richness and evenness relationships within Shannon–Wiener index values. *Ecological Indicators*, *67*, 703–713.
Szathmary, P. L., Helmuth, B., & Wethey, D. S. (2009). Climate change in the rocky intertidal zone: Predicting and measuring the body temperature of a keystone predator. *Marine Ecology Progress Series*, *374*, 43–56.
Thiel, M., & Ullrich, N. (2002). Hard rock versus soft bottom: The fauna associated with intertidal mussel beds on hard bottoms along the coast of Chile, and considerations on the functional role of mussel beds. *Helgoland Marine Research*, *56*, 21–30.
Thyrring, J., & Peck, L. S. (2021). Global gradients in intertidal species richness and functional groups. *eLife*, *10*, e64541.
Tokeshi, M., & Romero, L. (2000). Spatial overlap and coexistence in a mussel-associated Polychaete assemblage on a south American rocky shore. *Marine Ecology*, *21*, 247–261.
Torroglosa, M. E., & Giménez, J. (2018). Size at first maturity of Brachidontes rodriguezii (d'Orbigny, 1846) from the South-Western Atlantic Ocean. *Journal of the Marine Biological Association of the United Kingdom*, *98*, 457–462.
Ugland, K. I., Gray, J. S., & Ellingsen, K. E. (2003). The species–accumulation curve and estimation of species richness. *Journal of Animal Ecology*, *72*, 888–897.
Underwood, A. J., & Jernakoff, P. (1984). The effects of tidal height, wave-exposure, seasonality and rock-pools on grazing and the distribution of intertidal macroalgae in New South Wales. *Journal of Experimental Marine Biology and Ecology*, *75*, 71–96.
Valdivia, N., Aguilera, M. A., & Broitman, B. R. (2021). High dimensionality of the stability of a marine benthic ecosystem. *Frontiers in Marine Science*, *7*, 569650.
Valdivia, N., López, D. N., Fica-Rojas, E., Catalán, A. M., Aguilera, M. A., Araya, M., Betancourtt, C., Burgos-Andrade, K., Carvajal-Baldeon, T., Escares, V., Gartenstein, S., Grossmann, M., Gutiérrez, B., Kotta, J., Morales-Torres, D. F., Riedemann-Saldivia, B., Rodríguez, S. M., Velasco-Charpentier, C., Villalobos, V. I., & Broitman, B. R. (2021). Stability of rocky intertidal communities, in response to species removal, varies across spatial scales. *Oikos*, *130*, 1385–1398.
Whittaker, R. H. (1972). Evolution and measurement of diversity. *Taxon*, *21*(2/3), 215–251.
Wilbur, L., Küpper, F. C., Katsiaras, N., & Louca, V. (2023). Predicting diversity in benthic macro-scale communities associated with mussel matrices in three Pacific ecoregions. *Marine Ecology*, *44*(2), e12741.
Williams, S. E., Shoo, L. P., Isaac, J. L., Hoffmann, A. A., & Langham, G. (2008). Towards an integrated framework for assessing the vulnerability of species to climate change. *PLoS Biology*, *6*, e325.
Zhou, X. H., & Dinh, P. (2005). Nonparametric confidence intervals for the one- and two-sample problems. *Biostatistics*, *6*, 187–200.

SUPPORTING INFORMATION

Additional supporting information can be found online in the Supporting Information section at the end of this article.

How to cite this article: Wilbur, L., Küpper, F. C., & Louca, V. (2024). Algal cover as a driver of diversity in communities associated with mussel assemblages across eastern Pacific ecoregions. *Marine Ecology*, *45*, e12785. https://doi.org/10.1111/maec.12785